PERGAMON

Deep-Sea Research II 47 (2000) 3451–3490

DEEP-SEA RESEARCH
PART II

www.elsevier.com/locate/dsr2

Short-lived thorium isotopes (^{234}Th, ^{228}Th) as indicators of POC export and particle cycling in the Ross Sea, Southern Ocean

J.K. Cochran[a,*], K.O. Buesseler[b], M.P. Bacon[b], H.W. Wang[a], D.J. Hirschberg[a], L. Ball[b], J. Andrews[b], G. Crossin[b], A. Fleer[b]

[a]*Marine Sciences Research Center, State University of New York, Stony Brook, NY 11794-5000, USA*
[b]*Department of Marine Chemistry and Geochemistry, Woods Hole Oceanographic Institution, Woods Hole, MA 02543, USA*

Received 30 August 1999; received in revised form 15 February 2000; accepted 15 March 2000

Abstract

Repeated measurements of depth profiles of ^{234}Th (dissolved, 1–70 and >70 μm particulate) at three stations (Orca, Minke, Sei) in the Ross Sea have been used to estimate the export of Th and particulate organic carbon (POC) from the euphotic zone. Sampling was carried out on three JGOFS cruises covering the period from October 1996 (austral early spring) to April 1997 (austral fall). Deficiencies of ^{234}Th relative to its parent ^{238}U in the upper 100 m are small during the early spring cruise, increase to maximum values during the summer, and decrease over the course of the fall. Application of a non-steady-state model to the ^{234}Th data shows that the flux of Th from the euphotic zone occurs principally during the summer cruise and in the interval between summer and fall. Station Minke in the southwestern Ross Sea appears to sustain significant ^{234}Th removal for a longer period than is evident at Orca or Sei. Particulate ^{234}Th activities and POC are greater in the 1–70 μm size fraction, except late in the summer cruise, when the >70 μm POC fraction exceeds that of the 1–70 μm fraction. The POC/^{234}Th ratio in the >70 μm fraction exceeds that in the 1–70 μm fraction, likely due in part to the greater availability of surface sites for Th adsorption in the latter. Particulate ^{234}Th fluxes are converted to POC fluxes by multiplying by the POC/^{234}Th ratio of the >70 μm fraction (assumed to be representative of sinking particles). POC fluxes calculated from a steady-state Th scavenging model range from 7 to 91 mmol C m^{-2} d^{-1} during late January–early February, with the greatest flux observed at station Minke late in the cruise. Fluxes estimated with a non-steady-state Th model are 85 mmol C m^{-2} d^{-1} at Minke (1/13–2/1/97) and 50 mmol

* Corresponding author. Fax: 1-631-632-8820.
E-mail address: kcochran@notes.cc.sunysb.edu (J.K. Cochran).

0967-0645/00/$ - see front matter
PII: S0967-0645(00)00075-8

$C\,m^{-2}\,d^{-1}$ at Orca (1/19–2/1/97). The decline in POC inventories (0–100 m) is most rapid in the southern Ross Sea during the austral summer cruise (Smith et al., 2000. The seasonal cycle of phytoplankton biomass and primary productivity in the Ross Sea, Antarctica. Deep-Sea Research 47, 3119–3140; Gardner et al., 2000. Seasonal patterns of water column particulate organic carbon and fluxes in the Ross Sea, Antarctica. Deep-Sea Research II 47, 3423–3449), and the ^{234}Th-derived POC fluxes indicate that the sinking flux of POC is $\sim$ 30–50% of the POC decrease, depending on whether steady-state or non-steady-state Th fluxes are used. Rate constants for particle POC aggregation and disaggregation rates are calculated at station Orca by coupling particulate ^{234}Th data with ^{228}Th data on the same samples. Late in the early spring cruise, as well as during the summer cruise, POC aggregation rates are highest in near-surface waters and decrease with depth. POC disaggregation rates during the same time generally increase to a maximum and are low at depth ($>$ 200 m). Subsurface aggregation rates increase to high values late in the summer, while disaggregation rates decrease. This trend helps explain higher values of POC in the $>$ 70 m fraction relative to the 1–70 m fraction late in the summer cruise. Increases in disaggregation rate below 100 m transfer POC from the large to small size fraction and may attenuate the flux of POC sinking out of the euphotic zone.

1. Introduction

Productivity in high latitudes is characterized by extreme seasonal fluctuations due to light limitation and ice cover. In such areas, polynyas constitute sites in which productivity increases earlier than in surrounding ice-covered regions, and they may serve as net sinks for uptake of atmospheric CO_2 (Yager et al., 1995). The Ross Sea of the Southern Ocean is characterized by the development of a recurrent coastal polynya that opens initially close to the Ross Ice Shelf and develops northward. This area is a locus of biogenic silica formation and deposition, but relatively small amounts of organic carbon are stored in sediments there (Ledford-Hoffman et al., 1986; DeMaster et al., 1992; DeMaster et al., 1996; Nelson et al., 1996). The phytoplankton community in the Ross Sea is characterized by species of diatoms and dinoflagellates as well as the non-siliceous prymnesiophyte *Phaeocystis antarctica* (Leventer and Dunbar, 1996; Mathot et al., 1999). A principal focus of the Joint Global Ocean Study (JGOFS) Southern Ocean study is quantifying seasonal variations in carbon cycling in the Ross Sea and Antarctic Polar Front. The JGOFS cruises to the Ross Sea in 1996 and 1997 documented strong seasonal variations in primary production and phytoplankton biomass (Smith et al., 2000), as well as dissolved and particulate organic carbon (DOC, POC) inventories in the upper water column (Carlson et al., 2000; Gardner et al., 2000). The export of POC from the euphotic zone is an important component of the oceanic carbon cycle and provides a link between production and remineralization of organic matter in the upper water column and the burial of carbon in bottom sediments.

Short-lived thorium isotopes that are produced in the water column from dissolved parents and then subsequently attach to particles have proven useful in quantifying POC fluxes from the euphotic zone in a number of oceanic settings (e.g. Coale and Bruland, 1987; Buesseler et al., 1992a, 1995, 1998; Bacon et al., 1996; Cochran et al.,

1995; Charette and Moran, 1999; Murray et al., 1989, 1996; Langone et al., 1997) as well as the dynamics of sinking particles (Clegg and Whitfield, 1991; Clegg et al., 1991; Cochran et al., 1993; Murnane et al., 1994, 1996; Dunne et al., 1997). In particular, ^{234}Th (half-life = 24.1 d), produced from decay of dissolved ^{238}U, has been used as a proxy for POC flux. Thorium-234, coupled with ^{228}Th (half-life = 1.9 y) produced from decay of dissolved ^{228}Ra, has been used to calculate exchanges between particulate reservoirs via aggregation and disaggregation processes (Cochran et al., 1993; Murnane et al., 1996). Our goals in this paper are to use water column distributions of particulate and dissolved ^{234}Th and ^{228}Th to determine (1) seasonal variations of POC export from the euphotic zone and (2) particle cycling rates in the Ross Sea.

2. Methods

2.1. Sample collection

Samples were taken during three JGOFS cruises to the Ross Sea: early in the austral spring (10/2/96–11/8/96), in summer (1/13/97–2/11/97), and in autumn (3/31/97–5/14/97). Three sampling sites-Orca, Minke and Sei-were sampled repeatedly during the cruises (Fig. 1). Stations Orca and Minke provide endpoints for the JGOFS AESOPS sampling transect (Fig. 1), along which parameters such as

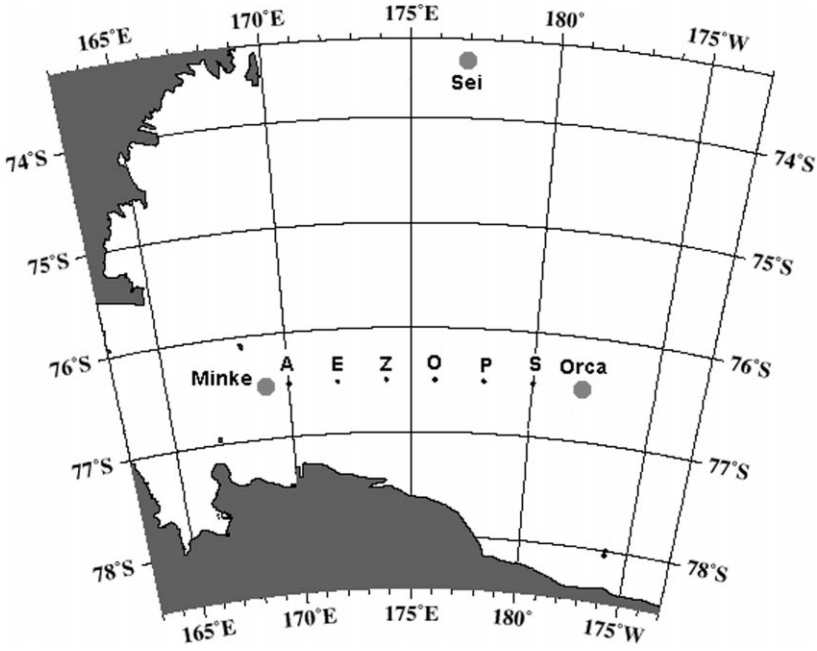

Fig. 1. Map of the Ross Sea showing station locations. The AESOPS transect in the southern Ross Sea is indicated.

production and biomass were repeatedly measured during the cruises (Smith et al., 2000).

Samples were collected by in situ pumping using battery-operated pumps that filter large volumes of water (100–1000 l) through a series of filters (Livingston and Cochran, 1987; Buesseler et al., 1992b). Particles were collected on two 142-mm diameter filters in a series consisting of a 70-μm pore sized Teflon mesh filter followed by a 1-μm pore-sized Microquartz filter. Dissolved Th was extracted onto two manganese oxide-impregnated wound fiber filter cartridges (Hytrex, nominal 0.5 μm). Flow rates were 4–8 l min^{-1}. In order to determine POC on the large size fraction, particles were rinsed off the Teflon filter using filtered seawater and refiltered onto 25-mm diameter silver filters (Buesseler et al., 1998).

2.2. Sample analyses

Activities of ^{234}Th on the manganese adsorber cartridges were determined mostly at sea using non-destructive gamma spectrometry. The cartridges were dried, crushed in a press to a cylindrical geometry and the 63 keV ^{234}Th gamma emission was counted using 1000- or 2000-mm^2 intrinsic germanium detectors (Buesseler et al., 1992b; Bacon et al., 1996). Extraction of ^{238}U from seawater is negligible on the manganese cartridges, and consequently no corrections were made for ingrowth of ^{234}Th. Thorium-234 in the particulate fractions was determined using non-destructive beta counting. Errors are calculated from 1σ counting error, including appropriate calibration errors. A subsample of the 1-μm Microquartz filter (approximately 50% of the 142-mm filter) was counted, while all the Ag filters resulting from rinsing the Teflon filters were measured. The filters were counted several times over three to four half-lives of ^{234}Th to correct for blank or long-lived beta activities present in the filters. Standardization of the various counting methods was accomplished by radiochemical analyses of selected samples for ^{234}Th (Buesseler et al., 1998). Filters or ashed cartridges were dissolved in HNO_3 and HCl, with ^{230}Th added as a yield monitor. Following purification of the Th fraction by ion exchange chromatography, Th was electrodeposited onto stainless-steel planchets and ^{234}Th was measured by beta counting.

Estimates of the rinsing efficiency of the Teflon filters were made by measuring the ^{234}Th remaining on the filters after rinsing. On average, $75 \pm 5\%$ of the Th was rinsed off the Teflon filter. We view this as the efficiency with which particles are physically removed from the Teflon filter by rinsing and have used it to correct both the ^{234}Th and POC data accordingly. Because the > 70-μm fraction is a small percentage of the total ^{234}Th, the rinsing efficiency correction has a negligible effect on the total ^{234}Th activity. It also should be noted that less than 100% rinsing efficiency of the Teflon filters does not affect the POC/^{234}Th ratio used to calculate POC fluxes.

Thorium-228 was measured by alpha spectrometry (Buesseler et al., 1992b; Cochran et al., 1993). Samples were dissolved in HNO_3, and Th was separated radiochemically using anion exchange chromatography. For the Ag filters, Ag was separated in a final anion exchange step using a 0.1 N HCl anion exchange column. The effluent from the first ion exchange column contained any Ra present and was saved to correct

for ^{228}Th ingrowth from ^{228}Ra between sample collection and initial ^{228}Th separation. ^{228}Ra was present in significant activities only on the manganese cartridges and ingrowth corrections were made for these samples. Ingrowth of ^{228}Th from ^{228}Ra was about 10% of the measured ^{228}Th in these samples.

POC and PON were measured on aliquots of the Microquartz and Ag filters using a CHNS analyzer. Carbonate was removed from the filter before analysis by fuming the filter with HCl.

3. Results

Dissolved ^{234}Th and ^{228}Th activities were calculated from the manganese cartridges. Generally, both the first and second cartridges were analyzed for ^{234}Th, whereas only the first cartridge was analyzed for ^{228}Th. The extraction efficiency (E) was determined from (Livingston and Cochran, 1987)

$$E = 1 - (\mathrm{MnB}/\mathrm{MnA}), \tag{1}$$

where MnA and MnB are the ^{234}Th activities on the first and second cartridges, respectively. Average values of E were 66.8 ± 27.4, 73.9 ± 12.7 and 72.7 ± 9.7% for the early spring, summer and fall cruises, respectively. Dissolved Th ($\mathrm{Th_d}$) was calculated as

$$\mathrm{Th_d} = \mathrm{MnA}/(E \times V), \tag{2}$$

where V is the volume filtered.

In approximately one-quarter of the samples, the extraction efficiency was anomalously low ($< 50\%$). We believe that these low efficiencies were due to the formation of ice crystals when the distilled water-saturated cartridges contacted cold air or sea water. Formation of ice could prevent dissolved Th from contacting the Mn oxide surfaces of the cartridges and adsorbing. Although the formally calculated efficiencies had large errors in these cases, the ^{234}Th activities were often readily measurable. We have attempted to estimate the dissolved activities in these samples as follows:

A lower estimate can be derived from the total ^{234}Th on the two cartridges. This is the minimum dissolved ^{234}Th contained in the sample and is calculated as

$$\mathrm{Th_d} = (\mathrm{MnA} + \mathrm{MnB})/V. \tag{3}$$

A higher estimate is obtained by dividing the result in Eq. (3) by the average efficiency obtained for the cruise:

$$\mathrm{Th_d} = (\mathrm{MnA} + \mathrm{MnB})/(E_{\mathrm{avg}} \times V). \tag{4}$$

As our "best estimate" of the dissolved ^{234}Th activity in these samples, we use the average of the results obtained from Eqs. (3) and (4). The "uncertainty" on these activities is taken as one-half the range between the values.

Dissolved ^{228}Th was calculated using Eq. (2) with the value of E obtained from the ^{234}Th data. For samples with low extraction efficiency, dissolved ^{228}Th was estimated from

$$^{228}\mathrm{Th}_{\mathrm{d}} = {}^{234}\mathrm{Th}_{\mathrm{d}}(228/234), \tag{5}$$

where (228/234) is the ^{228}Th/^{234}Th activity ratio on the MnA cartridge and $^{234}\mathrm{Th}_{\mathrm{d}}$ is the average obtained from Eqs. (3) and (4).

The thorium isotope data are available on the JGOFS Web site (http://www1.whoi.edu/jgdms_info.html) and are shown in Figs. 2a–c. Total ^{234}Th activities at Orca and Minke show near-equilibrium with ^{238}U during the early spring (Figs. 2a and b). Deficiencies increase during summer and decrease again by the fall. ^{228}Th profiles at station Orca (Fig. 3) show relatively little variation with depth during the spring, with a pronounced decrease of total activities in the upper 50–100 m during the summer cruise. Particulate ^{234}Th and ^{228}Th increase over the same time period, reaching highest values during the summer. Our values for total ^{228}Th are similar to those determined in the Weddell Sea (6–8 dpm/10^3 l) by Rutgers van der Loeff (1994). Radium-228 activities were not measured, but values in the Weddell Sea are 21–32 dpm/1000 l (Rutgers van der Loeff, 1994). We use these values only to indicate the likely magnitude of disequilibrium between ^{228}Th and ^{228}Ra, not to calculate scavenging rates or ^{228}Th deficiencies.

Thorium-234 activities in the 1–70 μm size fraction are always greater than those in the $>$ 70-μm fraction, often by factors of 10–20. The largest ^{234}Th activities in the $>$ 70-μm fraction are seen late in the summer cruise (Figs. 4a–c). Thorium-228 activities in the 1–70 μm fraction are usually greater than those in the $>$ 70-μm fraction, but in contrast to ^{234}Th, the disparity in the activities is not as large (Fig. 5).

POC concentrations show large variations with time (Fig. 6). The most complete temporal sequences are available at stations Orca and Minke and show progressive increases in POC in the upper 100 m from early spring to summer. Concentrations decrease from summer to fall. POC values in the 1–70 μm fraction are generally greater than those in the $>$ 70-μm fraction except late in the summer cruise when the situation is reversed. A pronounced subsurface maximum is also seen in the $>$ 70-μm POC concentrations at that time.

POC concentrations determined by large volume pumping in the Ross Sea can be an order of magnitude less than values determined on filtration of small volume ($\sim$ 1 l) samples from Niskin bottles (W. Gardner, pers. comm.; JGOFS database). Greater concentrations of POC and PON determined on small volume compared with large volume samples have been documented in previous studies (Altabet et al., 1992; Dunne et al., 1997; Moran et al., 1999). Moran et al. (1999) attributed such discrepancies to adsorption of DOC on the glass fiber filters used to filter the samples. This uncorrected blank is proportionately larger in smaller volume samples and can account for factors of 5–20 difference in the values when the POC (as sampled by pumps) is low ($\sim$ 1 μM). The study by Moran et al. (1999) used the same filter sizes for filtration of large- (in situ pump) and small-volume (bottle) samples, and hence concluded that correction for blanks caused by adsorption of DOC was necessary. Dunne et al. (1997) compared small-volume (bottle) POC measurements with samples

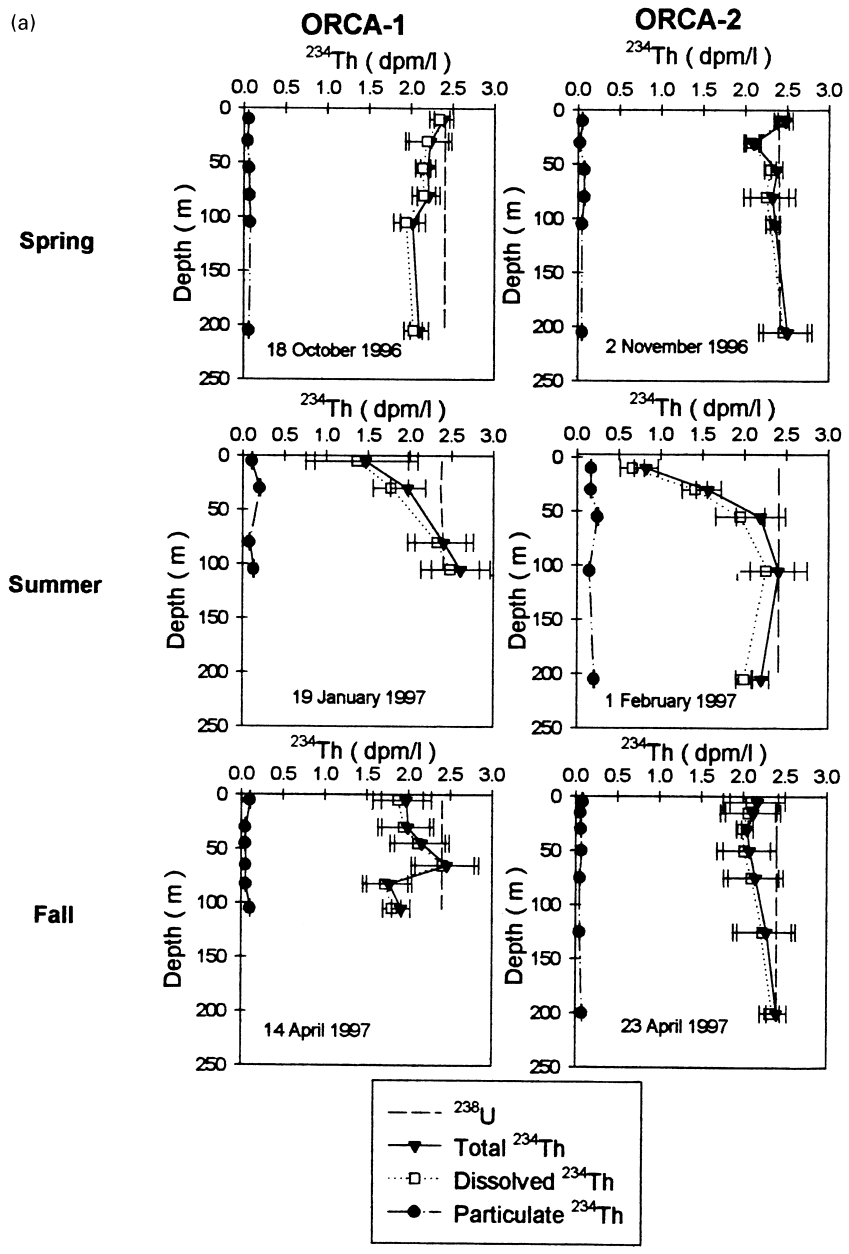

Fig. 2. Water column ^{234}Th profiles at stations Orca (a), Minke (b) and Sei (c). Particulate ^{234}Th is the sum of the $>$ 70 and 1–70 μm fractions. "Dissolved" ^{234}Th corresponds to that retained on manganese adsorber cartridges. Total ^{234}Th is the sum of particulate and dissolved Th. Dashed line corresponds to ^{238}U activity estimated from salinity (Chen et al., 1986). Designations " − 1" and " − 2" at the top of the figures refer to first and second occupations of a station on any given cruise.

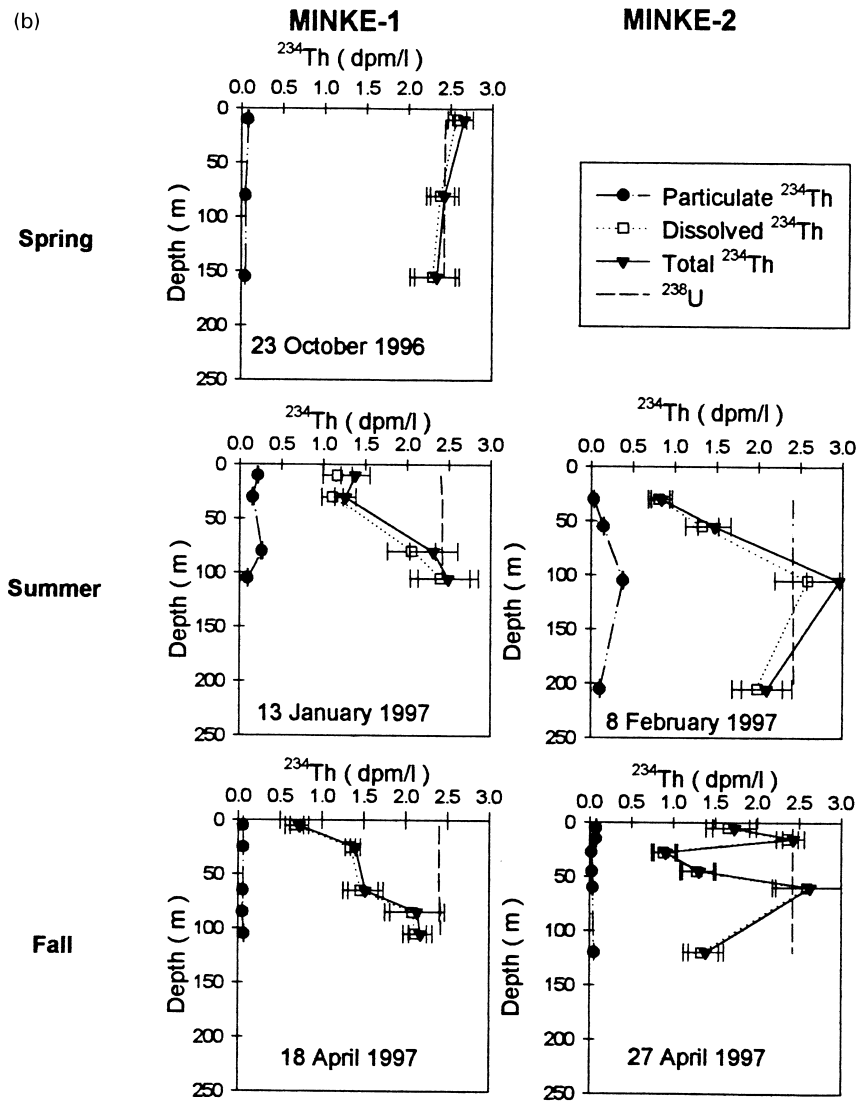

Fig. 2 (*continued*)

collected by in-situ pumping (MULVFS system of Bishop et al., 1985) and also noted greater values in the bottle samples. They observed that different filter sizes were used for the pump (>1 μm) and bottle (>0.6 μm) samples and concluded that submicron particles may not be sampled by the pumps. In the present case, the in-situ pumps used 1-μm Microquartz filters while the small volume samples were filtered using 0.7-μm glass fiber filters (Carlson et al., 2000). POC associated with particles smaller than 1 μm will not be retained on the pump filters. Moreover the higher pressure of

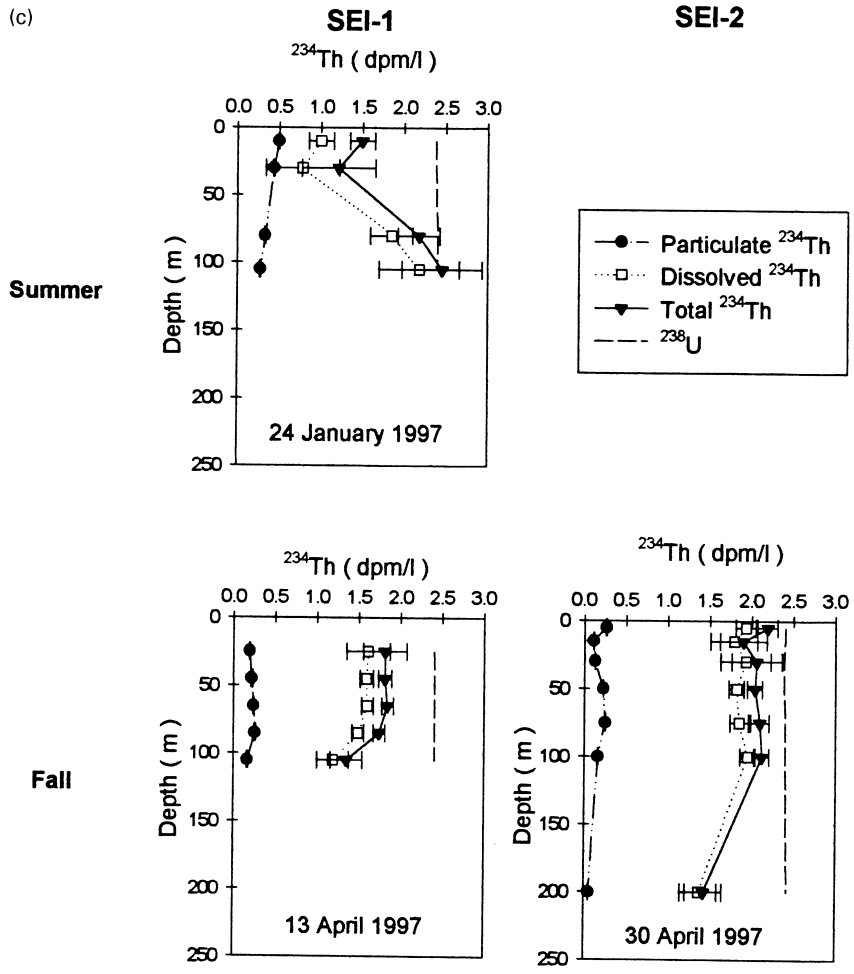

Fig. 2 (*continued*)

filtration on the in-situ pumps may force POC through the pump filters. By either explanation, the pump samples may be missing a fraction of the POC that is retained in the small-volume filtration of Niskin bottle samples. However, it is likely that any particles that pass the pump filters are retained on the manganese oxide sorber cartridges. Such a sampling artifact would underestimate particulate Th and overestimate dissolved Th. However the total ^{234}Th (particulate + "dissolved"), ^{234}Th deficiencies and POC/^{234}Th should not be affected. Indeed, the measurement of total ^{234}Th activities in equilibrium with ^{238}U in many samples in the present study is evidence of the accuracy of the collection of total ^{234}Th. The primary goal of this work is to estimate POC fluxes using the deficiency of total ^{234}Th with respect to ^{238}U, and this calculation should be unaffected by pump/bottle artifacts. However, the

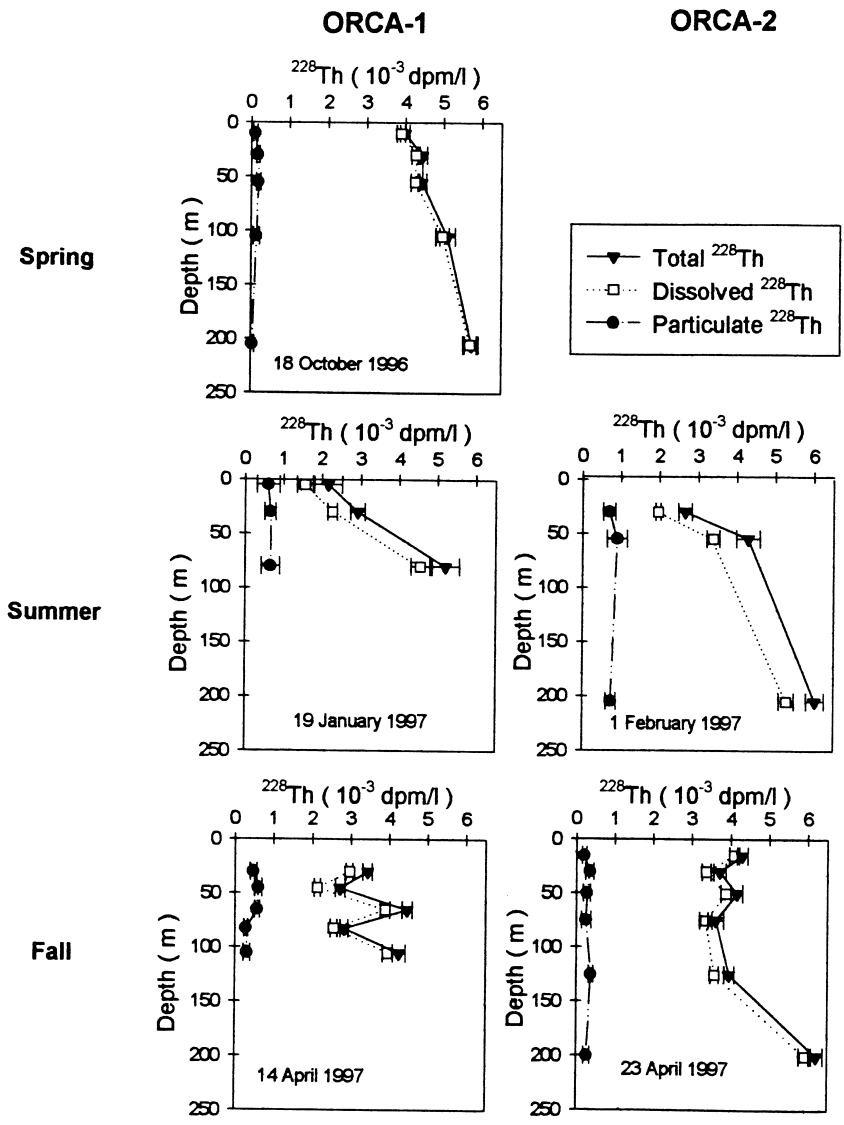

Fig. 3. Water column profiles of ^{228}Th at station Orca. Particulate ^{228}Th is sum of >70 and 1–70 μm fractions. Total ^{228}Th is sum of particulate and dissolved fractions.

discrepancy does reinforce the need to better intercompare the different methods and to make appropriate blank corrections to POC obtained from bottle samples.

Ratios of POC to ^{234}Th are generally greater in the >70-μm fraction than in the 1–70-μm fraction (Figs. 7a–c). Values increase with time, reaching maximum values during the summer. In most of the profiles, the POC/^{234}Th ratio is greatest in surface waters and decreases with depth, although subsurface maxima occur in a few profiles.

For purposes of calculating POC fluxes, we assume that the POC/^{234}Th ratio on the large particles is representative of that in the sinking flux. No shallow sediment traps were deployed during the JGOFS Southern Ocean study to provide samples of

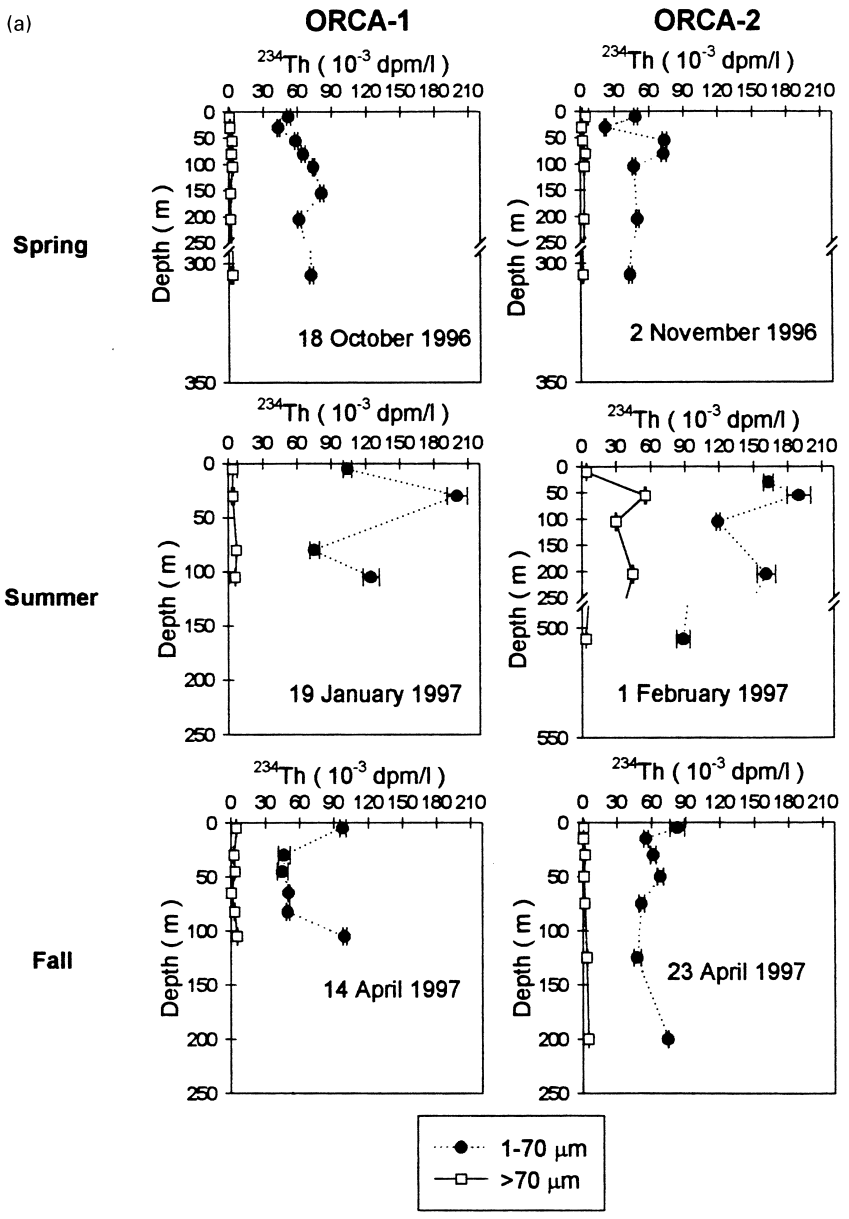

Fig. 4. Water column profiles of ^{234}Th in the 1– 70 and > 70 μm particulate fractions at stations Orca (a), Minke (b) and Sei (c).

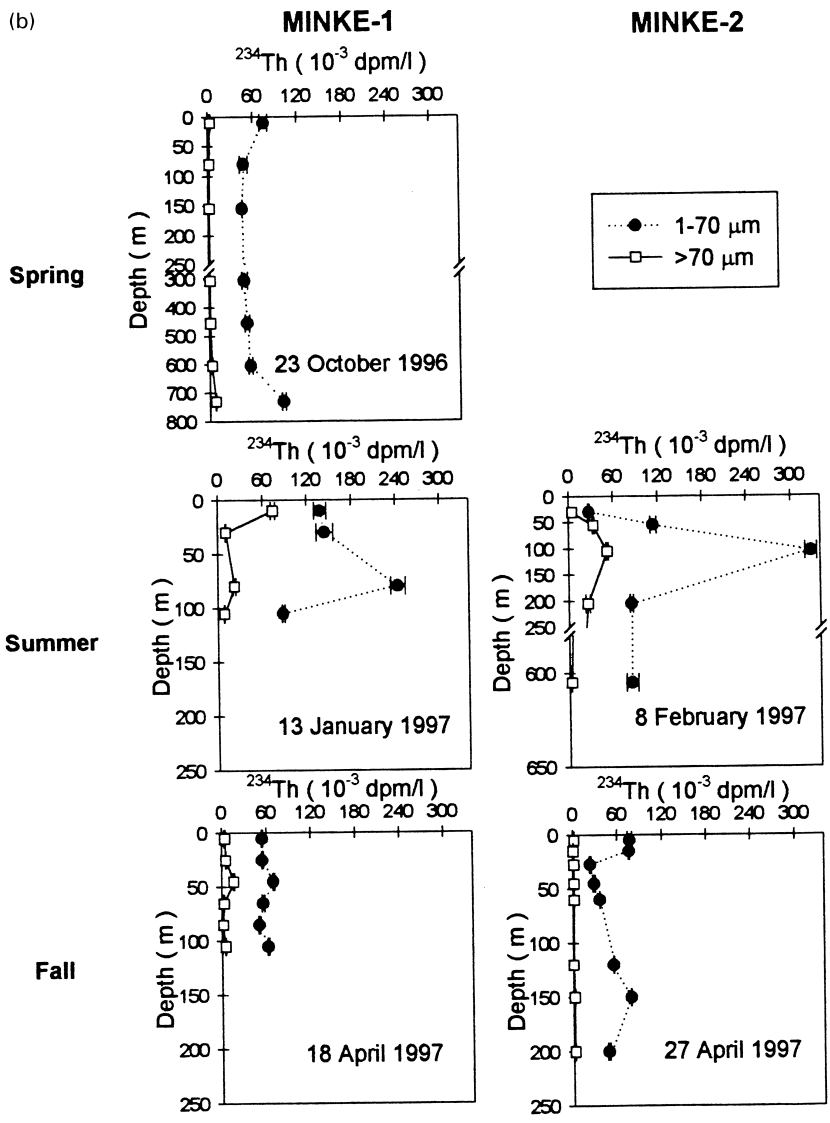

Fig. 4 (*continued*)

sinking particles that could be compared with the large particles collected by pumps. Moored traps were deployed at depth, but the recovery schedule of the moorings did not permit samples to be analyzed for ^{234}Th. Recent data collected in the Northwater Polynya (northern Baffin Bay) permits comparison of particles collected by pump with those collected by floating traps. These results show that POC/^{234}Th ratios on $>$ 70-μm particles collected with pumps at 100 m are within a factor of two of values

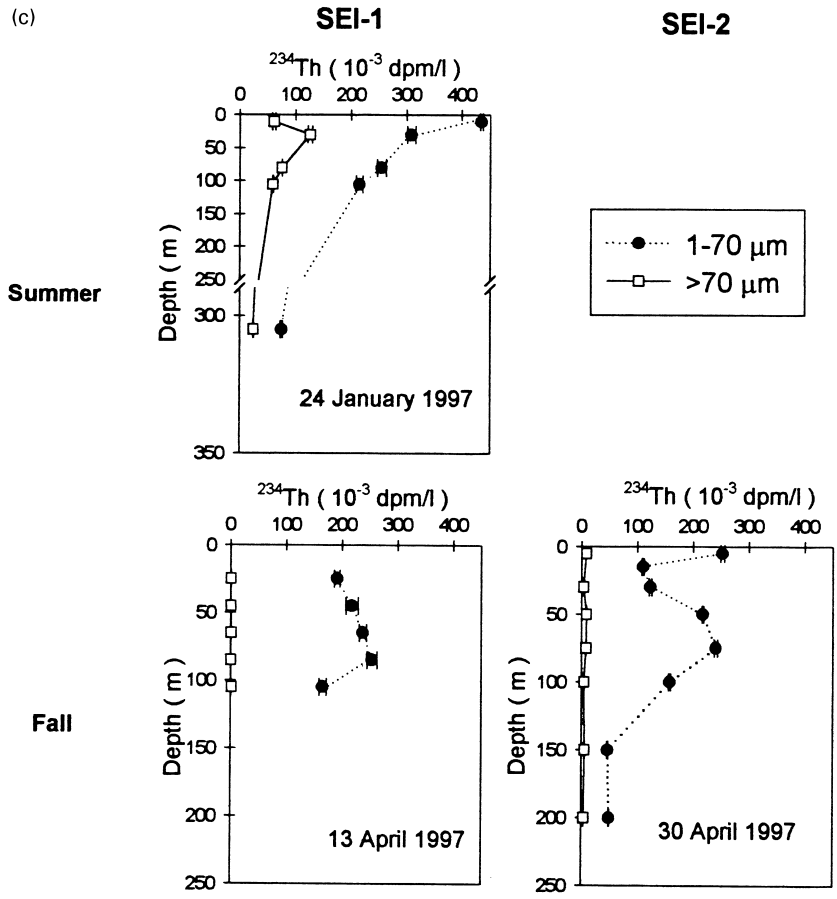

Fig. 4 (*continued*)

measured in floating trap material (Amiel and Cochran, unpublished data). Although we cannot test the reliability of the assumption that the POC/^{234}Th ratios of filtered large particles approximate those of sinking material in the Ross Sea, as noted by Bacon et al., (1996) this approach seems preferable to using the POC/^{234}Th values in bulk filtered particles.

4. Discussion

4.1. ^{234}Th and POC export from the euphotic zone

Scavenging of thorium onto sinking particles removes ^{234}Th from the oceanic water column. Simple box models have been used to express the mass balance of

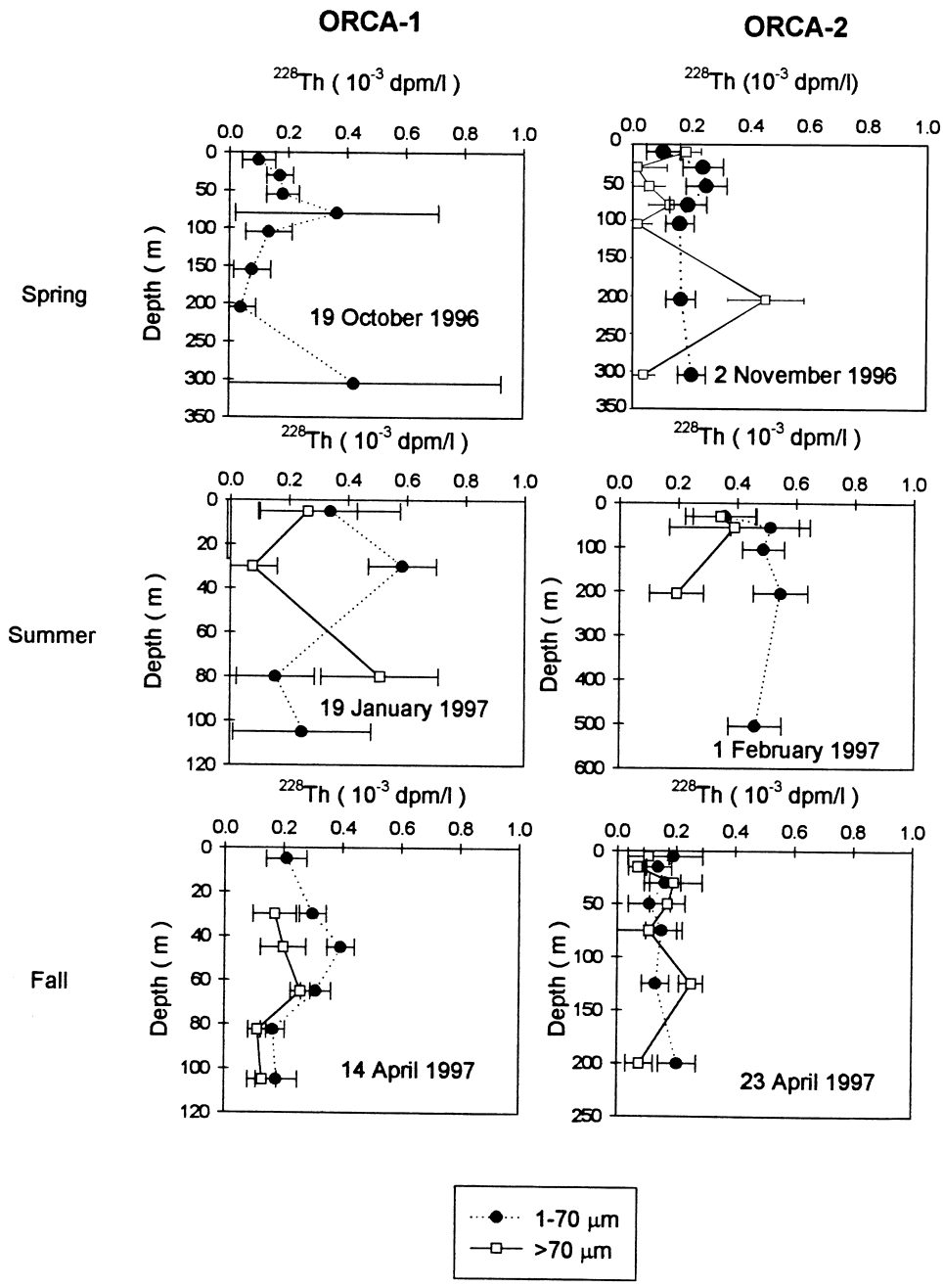

Fig. 5. Water column profiles of ^{228}Th in the 1–70 and >70 μm fractions at station Orca.

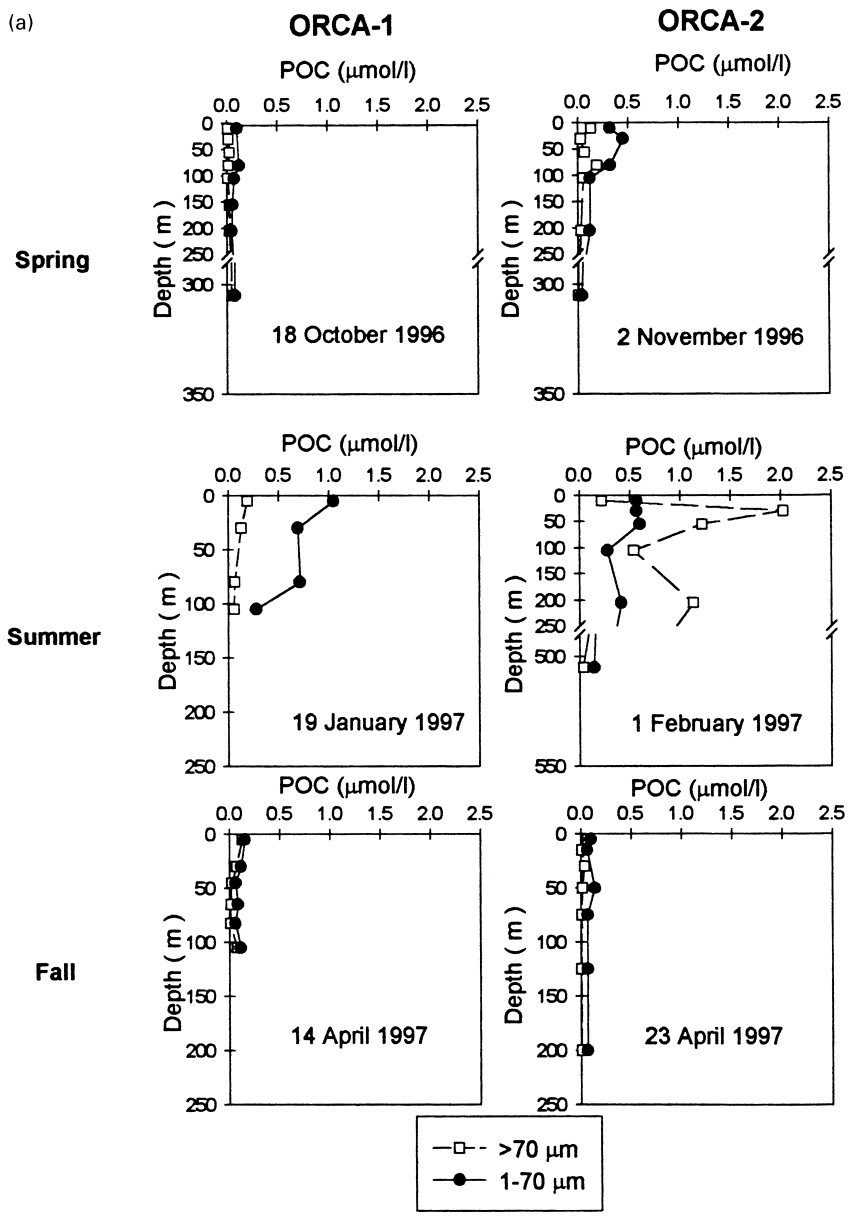

Fig. 6. Particulate organic carbon (POC) concentrations in 1–70 and >70 μm fractions sampled by in situ pumping at stations Orca (a), Minke (b) and Sei (c). Concentrations in the 1–70 μm fraction generally exceed those in the >70 μm fraction, except late in the summer cruise.

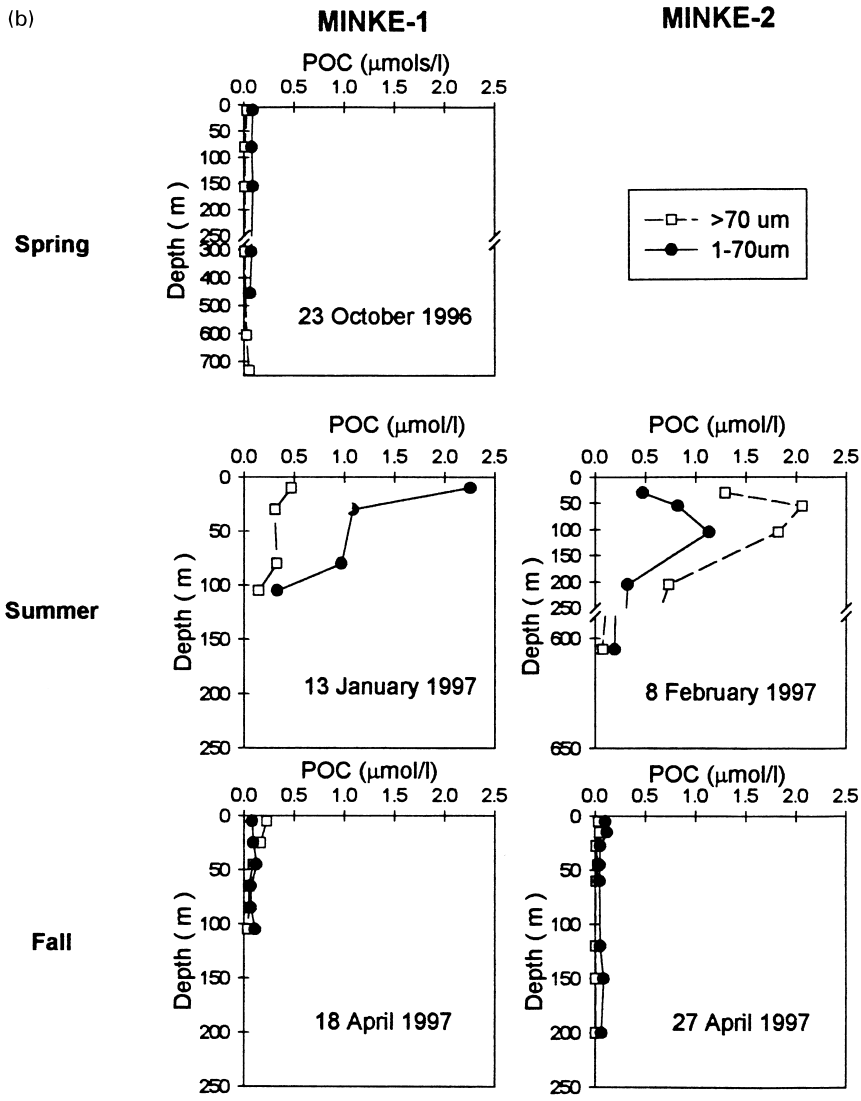

Fig. 6 (*continued*)

particulate ^{234}Th (Coale and Bruland 1987, Buesseler et al., 1992a):

$$\frac{\partial A_{\mathrm{tot}}}{\partial t} = [A_{\mathrm{U}} - (A_{\mathrm{p}} + A_{\mathrm{d}})]\lambda - P_{\mathrm{Th}} + V, \tag{6}$$

where $\partial A_{\mathrm{tot}}/\partial t$ is the temporal rate of change in total ^{234}Th (dissolved + particulate), A_{p} is particulate ^{234}Th, A_{d} is dissolved ^{234}Th, A_{U} is the ^{238}U activity, λ is the ^{234}Th

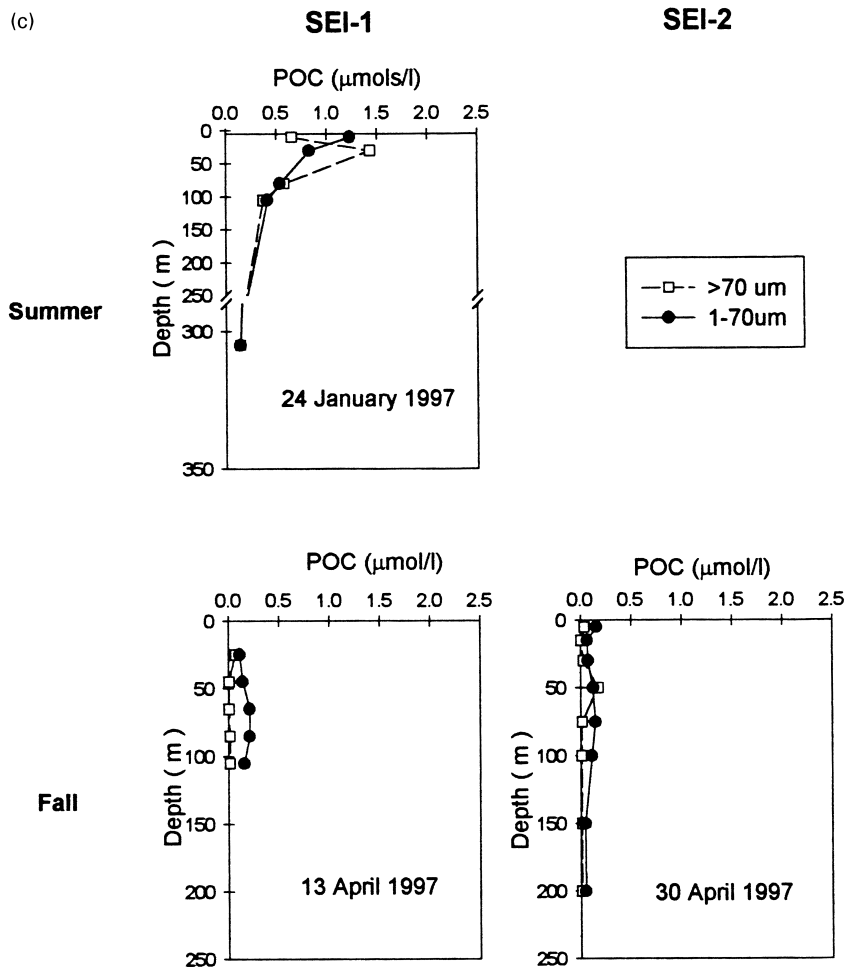

Fig. 6 (*continued*)

decay constant (0.0288 d^{-1}), P_{Th} is the net flux of ^{234}Th on particles sinking into and out of the box, and V represents transport of dissolved and particulate ^{234}Th by processes other than particle sinking (e.g. advection, eddy diffusion). Uranium-238 activities were determined from salinities (Chen et al., 1986).

The net sinking flux of ^{234}Th is given by

$$P_{Th} = (A_U - A_{tot})\lambda - \partial A_{tot}/\partial t + V, \tag{7}$$

If the removal flux of ^{234}Th is driven by local production and export of organic matter, fluxes of POC and other biogenic components can be calculated as

$$\text{POC flux} = (\text{POC/Th})_L P_{Th}, \tag{8}$$

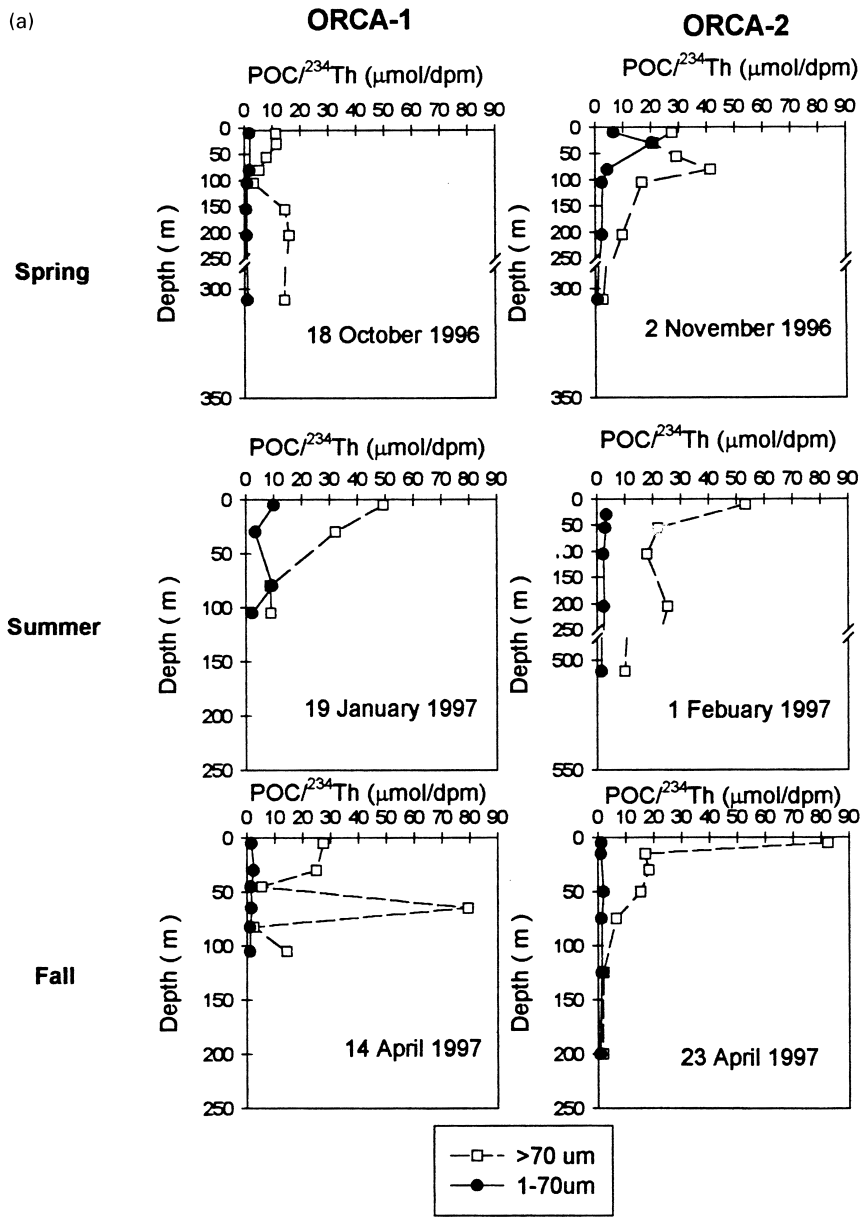

Fig. 7. POC/^{234}Th ratios in particles filtered in situ at stations Orca (a), Minke (b) and Sei (c). The $>$ 70 μm fraction is taken as representative of sinking material in flux calculations.

where $(POC/Th)_L$ is the ratio of POC (or other biogenic component) to ^{234}Th on sinking particles. The most complete estimate of P_{Th} in Eq. (7) requires both temporal and spatial measurements of ^{234}Th depth profiles. In the present case, we have at most

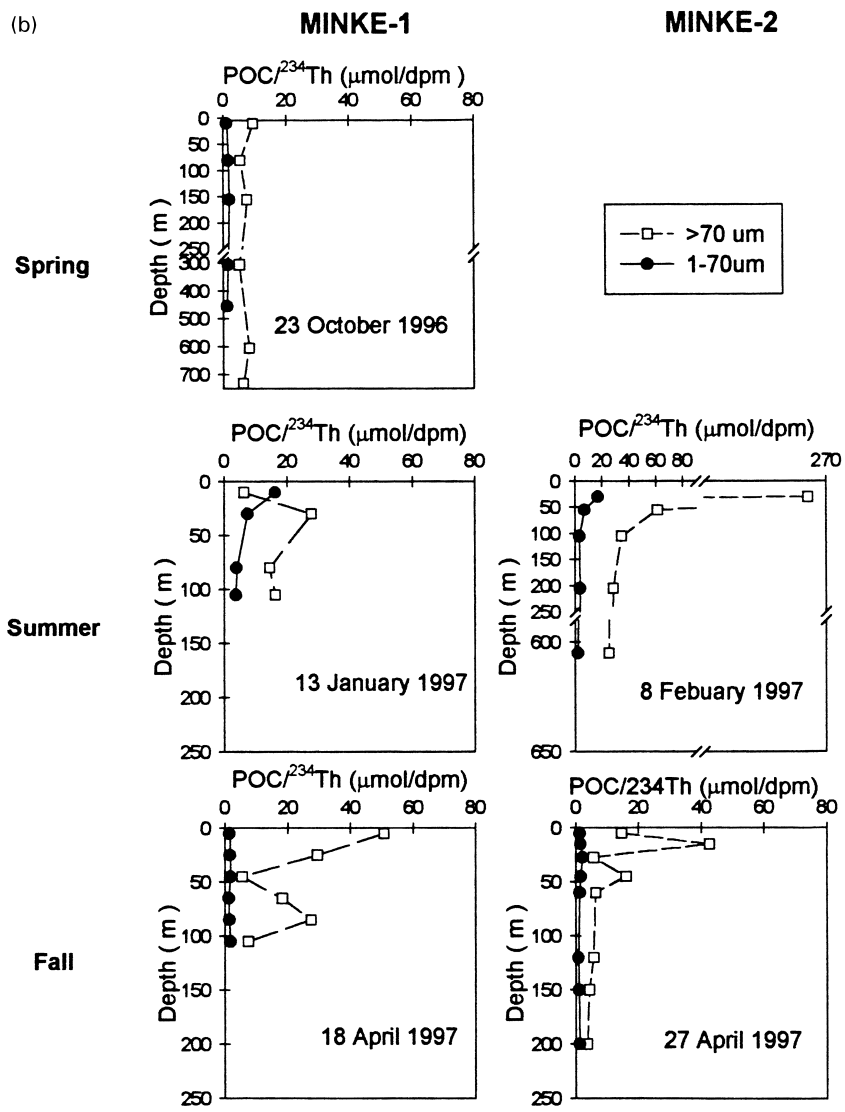

Fig. 7 (*continued*)

two occupations of a given station on each cruise, permitting some evaluation of the temporal term in Eq. (7).

The transport term, V, includes both horizontal and vertical diffusive and advective transport. In areas where upwelling is well developed, such as the equatorial Pacific, vertical advective transport of ^{234}Th can be significant. For example, Buesseler et al. (1995) and Bacon et al. (1996) observed that inclusion of upwelling in calculations of ^{234}Th export from the equatorial Pacific produced fluxes that were up to 40% greater

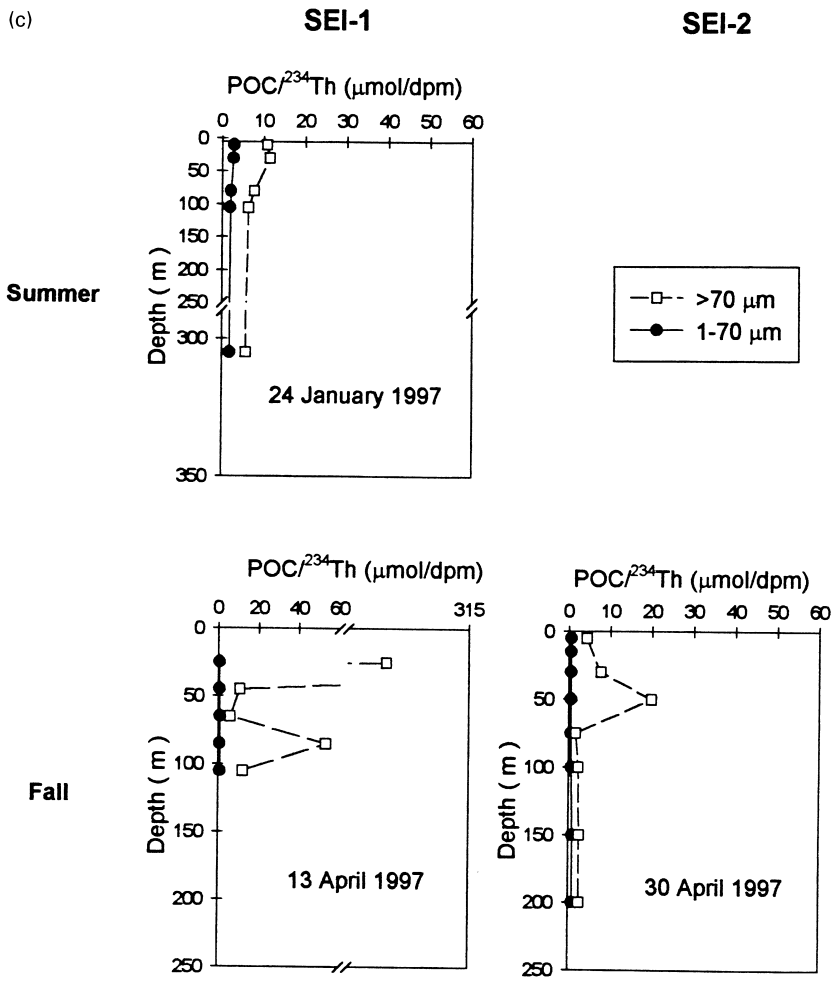

Fig. 7 (*continued*)

than those calculated without upwelling. In the Arabian Sea, the contribution of upwelling to the net ^{234}Th flux also can be significant (Buesseler et al., 1998). Upwelling is not well developed in the Ross Sea, and we assume its contribution to the ^{234}Th flux is small.

The effect of horizontal advective transport on ^{234}Th profiles and fluxes was shown to be small in the North Atlantic and Arabian Sea (Buesseler et al., 1992a, 1998). However, in coastal settings the impact of such transport can be larger. In the Northeast Water Polynya (East Greenland Shelf), Cochran et al. (1997) observed that ^{234}Th deficits measured at stations taken over distances of 80 km along the circulation of a small gyre increased in the downstream direction. Taking advective transport into account increased the calculated ^{234}Th flux by 70% relative to a model in which

advection was neglected. Gustafsson et al. (1998) showed that advection was important in estimating ^{234}Th export fluxes in inner Casco Bay, Gulf of Maine. In the outer bay, however, the impact was much less. In the case of the Gulf of Maine, the greatest contribution of advective transport of ^{234}Th was during times of reduced scavenging by local processes (Gustafsson et al., 1998).

Circulation in the Ross Sea is cyclonic, with westward flows in the southern portion and northward flows along the western margin (Jacobs et al., 1970; El-Sayed et al., 1983). If advective transport of water and particles does influence the water column ^{234}Th profiles in the Ross Sea, these circulation considerations suggest that the Th distributions at Orca could affect profiles at Minke, which in turn might influence profiles at Sei. Jaeger et al. (1996) conducted an extensive comparison of the dynamics of currents in the Ross Sea with the settling velocities of sinking particles to evaluate areas in which a one-dimensional (vertical) settling model was most appropriately applied to sediment trap and bottom sediment data. Their dynamic modeling shows that displacements during particle settling are < 20 km in the southwestern Ross Sea (closest to station Minke), < 50 km in the south-central area (close to station Orca) and > 50 km at a northwestern site (close to station Sei), relative to the time required for a particle to reach the bottom. These calculations use settling velocities of 50–200 m d^{-1}, and displacements would be larger for more slowly settling material. However, they also consider the whole water column, and displacements would be less if only the upper 100 m were considered. The distances between stations Orca, Minke and Sei are larger than the particle displacements calculated by Jaeger et al., (1996) for the southern Ross Sea, and we assume that the ^{234}Th profiles at Orca, Minke and Sei are minimally affected by advection (i.e. V is zero in Eq. (6)). Multiple profiles representing significant spatial coverage would be needed to evaluate this assumption more rigorously.

We begin an evaluation of POC export in the Ross Sea by calculating the flux required to support the observed ^{234}Th deficiency in the euphotic zone (effectively 100 m). This is calclulated from the integrated ^{234}Th deficiency to 100 m, $(A_U - A_{tot})\lambda$, and is obtained from Eq. (7) by setting the temporal and transport terms equal to zero. Such an approach is equivalent to assuming that the profiles are in a steady state with respect to production of ^{234}Th, decay and export of particulate ^{234}Th. Although ^{234}Th deficiencies may persist below 100 m, integrating the deficiency to 100 m gives the sinking flux of ^{234}Th passing that depth horizon. Export fluxes of ^{234}Th calculated in this fashion are low during the early spring cruise, increase with time during the summer cruise and decrease with time during the fall cruise (Fig. 8). Because station Sei was sampled only once during the summer cruise, we can not document increasing ^{234}Th removal with time at this station. However, as with the other stations, the trend at Sei during the fall is decreasing ^{234}Th deficiencies with time. The long time gap between the summer and fall cruises obscures the temporal trends in Th flux, but it appears that maximum fluxes occur late in the summer cruise or in the interval between the cruises. There are differences between stations, with fluxes greatest at Minke during both the summer and fall cruises.

The flux of ^{234}Th from the euphotic zone is driven by bulk fluxes because Th adsorbs onto the diversity of particles (biogenic and lithogenic) comprising the flux.

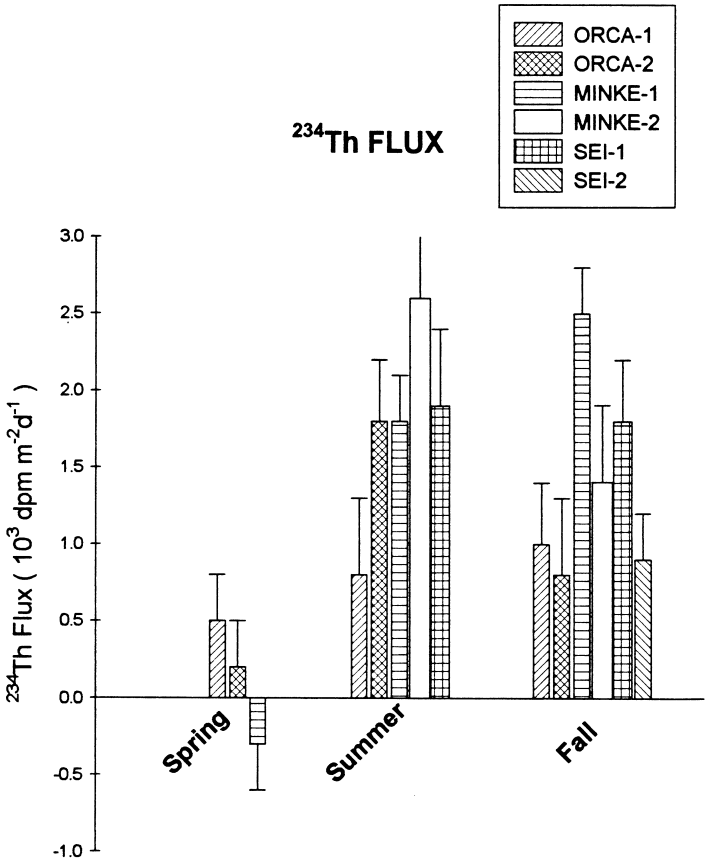

Fig. 8. ^{234}Th export from the upper 100 m determined by a steady-state Th scavenging model. The model assumes no temporal change or advective influences on the profiles of Fig. 2.

There are few measurements of particle flux from the upper water column with which to compare our ^{234}Th fluxes. Asper and Smith (1999) determined particle fluxes in the Ross Sea using arrays of floating sediment traps. Their data from 1995 to 1996 were collected in late December to mid-January, and most closely correspond to the seasonal timing of the JGOFS summer cruise. Asper and Smith (1999) observed bulk fluxes at 100 m in the southwestern Ross Sea that were greater by a factors of 1.3–1.6 compared with stations in the southeast. Such a difference can be explained by a dominance of rapidly sinking diatoms in the former case relative to more slowly sinking *Phaeocystis* colonies in the latter. The ^{234}Th fluxes at 100 m determined for the summer cruise reflect similar spatial differences in flux with greater values at station Minke relative to station Orca. Moored sediment traps were deployed during the JGOFS Southern Ocean Study, but at only two locations in the vicinity of stations Orca and Sei (Collier et al., 2000). Spatial differences are also apparent in these results, with both annual and summer bulk fluxes greater at the southern station.

POC fluxes can be determined from the ^{234}Th fluxes by multiplying the latter by the POC/Th ratio on sinking particles at 100 m. The errors on these flux estimates are based on propagation of the 1σ errors of the Th deficiencies and POC/Th ratios. As described above, we take the POC/Th ratio on the $>$ 70-μm particles as representative of that on sinking material. The POC fluxes calculated from the steady-state ^{234}Th export (Fig. 9) are low during the early spring, increase with time during the summer cruise and decrease toward the end of the fall cruise. The maximum flux recorded at station Minke (91 ± 3 mmol C m^{-2} d^{-1}; Table 1) is approximately three times that estimated at either Orca or Sei. At stations Orca and Minke, the POC fluxes at the start of the fall cruise are substantially reduced from maximum values late in the summer cruise. POC fluxes at station Sei early in the fall are comparable or greater than those late in the summer.

There is considerable prior evidence for distinct spatial patterns in productivity and POC flux in the Ross Sea that supports the trends seen in the ^{234}Th-derived POC fluxes. Smith et al. (1996) showed that biomass and productivity in the southern Ross Sea were greater than in the north. They linked these patterns to ice retreat, with ice disappearing from the south as the Ross Sea Polynya opens and from the north as the ice edge retreats toward the continental shelf edge. Within the southern Ross Sea, Nelson et al. (1996) showed that productivity was greatest in the southwest Ross Sea and peaked earlier than in the southeastern portion. Production in the southeastern Ross Sea was dominated by the non-siliceous *Phaeocystis antarctica* while diatoms dominated in the southwest, and as a consequence biogenic silica production was greatest in the southwest (Nelson et al., 1996). Fluxes of biogenic silica recorded in sediment traps at depth peaked earlier in the southwestern Ross Sea than in the southeastern portion (DeMaster et al., 1992). With respect to POC fluxes, Dunbar et al. (1998) presented sediment trap data that showed generally greater fluxes in the southeastern Ross Sea relative to the southwest. They also observed significant interannual variation and occasional reversals of this pattern. The productivity and POC data of Smith et al. (2000) and Gardner et al. (2000) from the JGOFS AESOPS transect in the Ross Sea show that productivity peaked approximately 30 days before POC standing crop, with the greatest decline in the latter occurring over the course of the summer cruise.

Depth profiles of POC flux can be determined in a manner similar to that for the euphotic zone by applying Eq. (7) to discrete depth intervals of the ^{234}Th profiles. In this case, the POC/^{234}Th ratio of the $>$ 70-μm particles at the base of a given depth interval is used to calculate POC export through that depth. These results show that during the summer cruise, fluxes decrease with depth from a subsurface maximum (Figs. 10a–c). Highest fluxes are seen at station Minke late in the summer cruise. The profiles indicate that, relative to the maximum values, 50–80% of the POC is remineralized within the upper 100 m, although these estimates are based on a steady-state interpretation of the ^{234}Th profiles (see below) and are likely to be upper limits. Our calculated POC flux profiles are qualitatively similar to those determined by Asper and Smith (1999) using floating trap arrays in the southern Ross Sea in December 1995 and January 1996. Their data show decreases in POC flux from 50 to 100 m (factors of 1.4–2) that are similar in magnitude to those estimated from the ^{234}Th data at stations Orca and Minke (Figs. 10a and b).

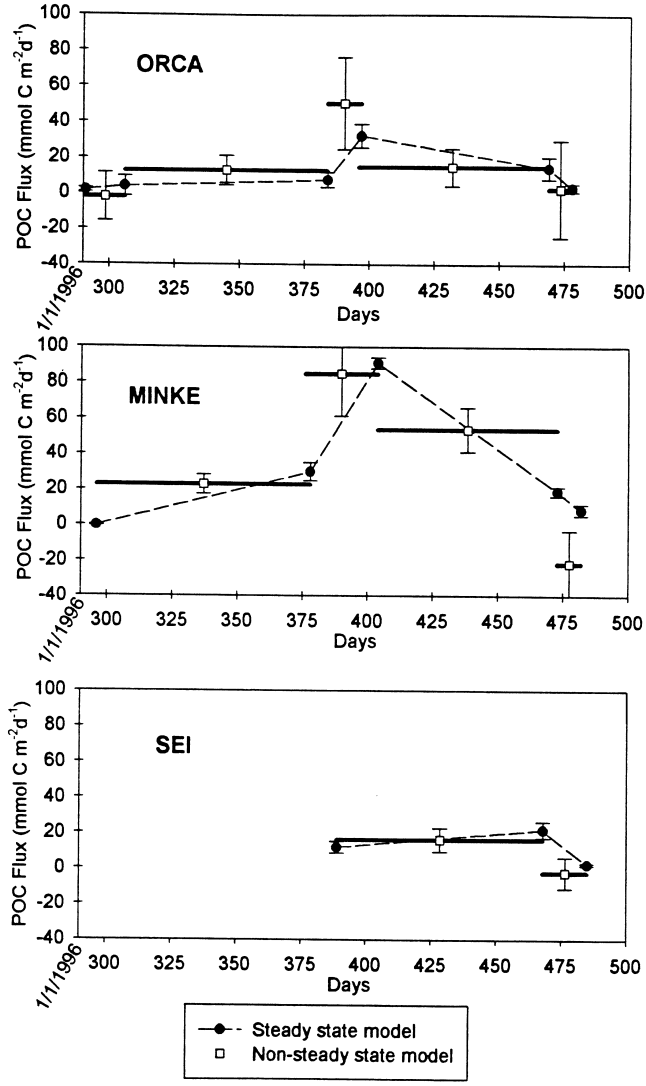

Fig. 9. POC fluxes at 100 m vs. time at stations Orca (a), Minke (b) and Sei (c). Values determined from the steady-state model use the ^{234}Th fluxes shown in Fig. 8, multiplied by the POC/^{234}Th ratio in the >70 μm particulate fraction at 100 m. Non-steady-state calculations are based on non-steady-state ^{234}Th fluxes determined by taking temporal change in the profiles into account. Horizontal bars on the non-steady-state fluxes correspond to the time interval over which the model is applied. Days correspond to year 1996 days.

An important aspect of the calculation of ^{234}Th export fluxes determined from water column profiles is that the profiles may not be at steady state and the left-hand side of Eq. (6) cannot be assumed to be zero. Buesseler et al. (1992a) pointed out that non-steady-state conditions would be expected to obtain in situations of a bloom in

Table 1
^{234}Th deficiencies (0–100 m), particulate ^{234}Th fluxes, POC and PON export fluxes at 100 m calculated from a steady-state Th scavenging model[a]

Cruise	Site	Sampling date[b]	^{234}Th deficit^{+} (10^3dpm m^{-2})	P_{Th} (10^3dpm m^{-2} d^{-1})	POC flux (mmol C m^{-2}d^{-1})	PON flux (mmol N m^{-2}d^{-1})
Spring	ORCA-1	10/18/96	17.6 ± 11.6	0.5 ± 0.3	1.6 ± 1.1	0.7 ± 0.4
	ORCA-2	11/02/96	8.0 ± 11.6	0.2 ± 0.3	3.9 ± 5.6	0.7 ± 1.0
	MINKE-1	10/23/96	− 9.9 ± 10.6	− 0.3 ± 0.3	− 1.7 ± 1.8	− 0.4 ± 0.4
Summer	ORCA-1	01/19/97	29.0 ± 16.4	0.8 ± 0.5	7.4 ± 4.2	2.6 ± 1.5
	ORCA-2	02/01/97	62.2 ± 12.8	1.8 ± 0.4	32.2 ± 6.6	4.1 ± 0.9
	MINKE-1	01/13/97	64.2 ± 11.0	1.8 ± 0.3	29.9 ± 5.1	4.2 ± 0.7
	MINKE-2	02/08/97	91.0 ± 13.0	2.6 ± 0.4	91.0 ± 3.0	8.3 ± 1.2
	SEI-1	01/24/97	66.4 ± 18.4	1.9 ± 0.5	11.9 ± 3.3	1.4 ± 0.4
Fall	ORCA-1	04/14/97	34.5 ± 15.1	1.0 ± 0.4	14.2 ± 6.2	0.9 ± 0.4
	ORCA-2	04/23/97	26.2 ± 17.7	0.8 ± 0.5	3.2 ± 2.2	0.8 ± 0.5
	MINKE-1	04/18/97	88.3 ± 12.1	2.5 ± 0.3	18.9 ± 2.6	3.6 ± 0.5
	MINKE-2	04/27/97	49.9 ± 18.6	1.4 ± 0.5	8.5 ± 3.2	2.6 ± 1.0
	SEI-1	04/13/97	62.8 ± 13.0	1.8 ± 0.4	21.7 ± 4.5	ND
	SEI-2	04/30/97	33.0 ± 10.3	0.9 ± 0.3	2.3 ± 0.7	0.75 ± 0.23

[a]ND: no data. + ^{234}Th deficit = $\{A_U - (A^d_{Th} + A^p_{Th})\}$ for 0–100 m.
[b]mm/dd/yy.

which the sinking flux from the euphotic zone is initially increasing and then decreasing, often on a time scale comparable to the half-life of ^{234}Th. At a minimum, these conditions are met during the summer cruise and in the interval between the summer and fall cruises, when the ^{234}Th profiles are changing substantially and the standing

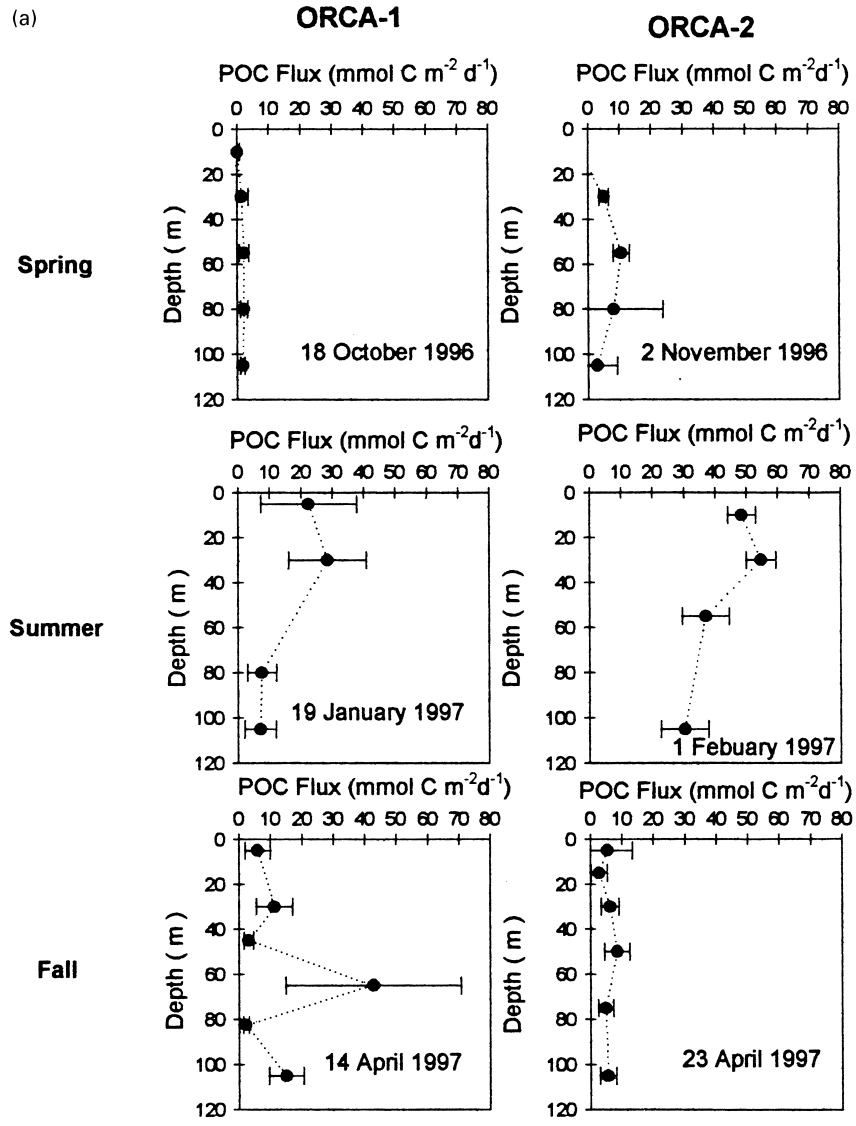

Fig. 10. Depth profiles of POC flux at Orca (a), Minke (b) and Sei (c), calculated by multiplying the steady-state ^{234}Th deficits for given depth intervals by the POC/^{234}Th ratio in the > 70 m size fraction (Fig. 7). Note attenuation of flux at stations Orca and Minke during the summer cruise.

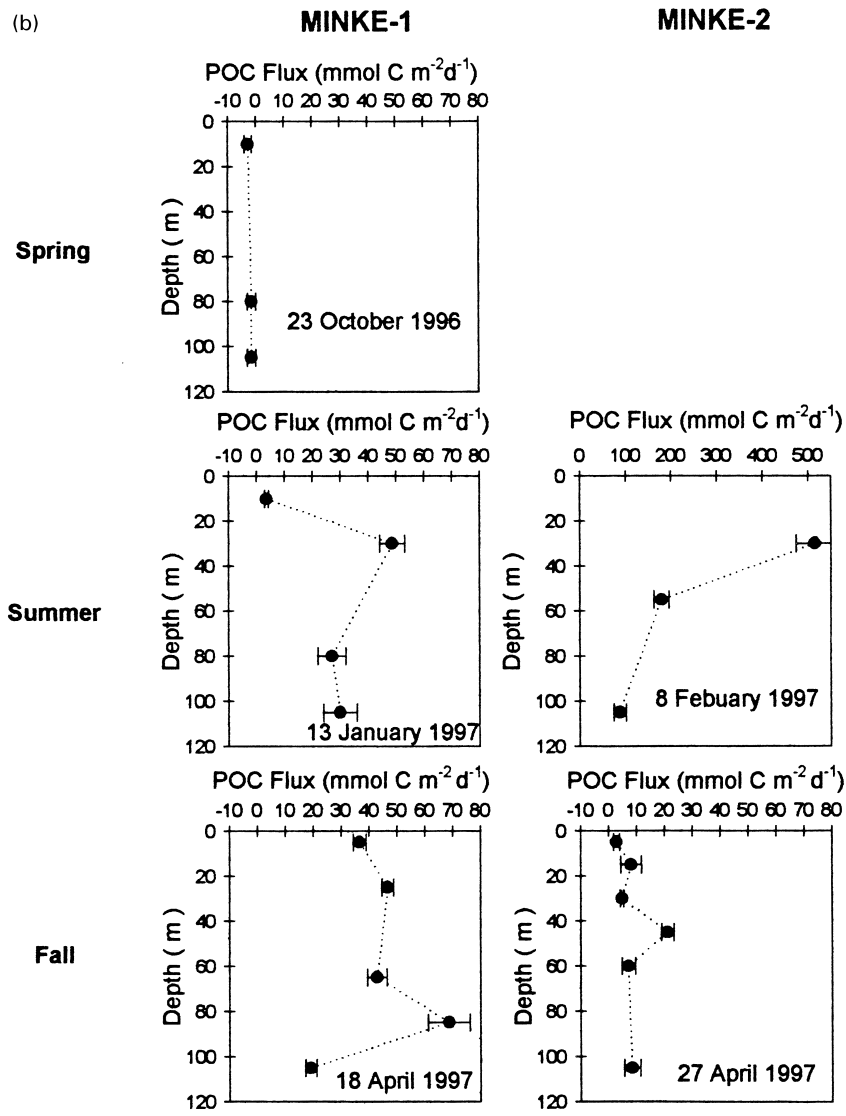

Fig. 10 (*continued*)

crop of POC shows the largest changes (Smith et al., 2000, Gardner et al., 2000). As shown by Buesseler et al. (1992a), taking temporal changes in the ^{234}Th profiles into account modifies Eq. (7) to

$$P_{\mathrm{Th}} = \lambda\left[\frac{A_{\mathrm{U}}(1-\mathrm{e}^{-\lambda t}) + A^{\mathrm{tot}}_{\mathrm{Th}-1}\mathrm{e}^{-\lambda t} - A^{\mathrm{tot}}_{\mathrm{Th}-2}}{(1-\mathrm{e}^{-\lambda t})}\right], \tag{9}$$

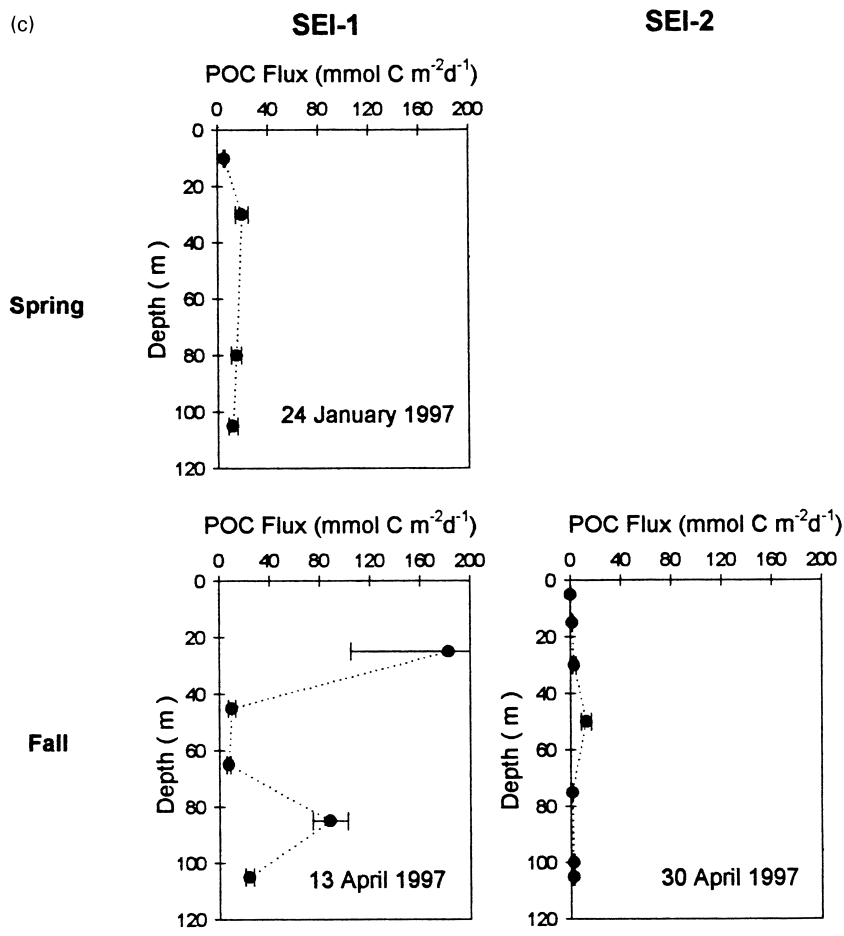

Fig. 10 (*continued*)

where A_U, $A^{tot}_{Th-1,2}$ are the integrated ^{238}U and total ^{234}Th activities in 0–100 m at times 1 and 2, and t is the time between profiles. Eq. (9) still assumes that the transport term (V) in Eq. (6) is negligible.

We are able to use Eq. (9) to evaluate the importance of temporal changes in the ^{234}Th profiles to the estimation of POC flux at station Orca during all three cruises, at Minke during the summer and fall and at Sei during the fall. Additional estimates can be made for the time intervals between the cruises. The error on P_{Th} calculated from Eq. (9) includes the propagation of errors in the Th inventories from the two profiles and is larger than that for P_{Th} calculated from a single profile. The results show that ^{234}Th export is significant during the summer and in the interval between the summer and fall cruises at Minke and Sei (Table 2). Indeed, if this were not the case, it is likely

Table 2
Particulate ^{234}Th, POC and PON fluxes at 100 m, calculated from a non-steady-state Th scavenging model[a]

Station	Austral season	Time interval (mm/dd/yy)	P_{Th} (dpm m^{2}d^{-1})	Average POC/^{234}Th (μmol dpm^{-1})	POC Flux (mmol Cm^{-2} d^{-1})	Average PON/^{234}Th (μmol dpm^{-1})	PON Flux (mmol Nm^{-2} d^{-1})
ORCA	Spring	10/18–11/2/96	-0.2 ± 1.3	10.0	-2.2 ± 13.5	2.19	-0.5 ± 2.9
	Spring → Summer	11/2/96–1/19/97	1.0 ± 0.6	12.8	12.6 ± 8.3	3.12	3.1 ± 2.0
	Summer	1/19–2/1/97	3.7 ± 1.9	13.5	50.3 ± 25.8	2.75	10.3 ± 5.3
	Summer → Fall	2/1–4/14/97	0.9 ± 0.6	16.2	14.7 ± 10.5	1.63	1.5 ± 1.1
	Fall	4/14–23/97	0.3 ± 2.9	9.3	2.5 ± 27.2	0.97	0.3 ± 2.8
MINKE	Spring → Summer	10/23/96–1/13/97	2.1 ± 0.5	11.1	22.8 ± 5.4	1.76	3.6 ± 0.8
	Summer	1/13–2/8/97	3.3 ± 0.9	25.5	84.9 ± 23.7	2.73	9.1 ± 2.5
	Summer → Fall	2/8–4/18/97	2.5 ± 0.6	21.1	53.6 ± 12.5	2.29	5.8 ± 1.4
	Fall	4/18–27/97	-3.2 ± 2.9	6.69	-21.7 ± 18.7	1.6	-5.2 ± 4.5
SEI	Summer → Fall	1/24–4/13/97	1.8 ± 0.7	9.11	16.1 ± 6.6	ND	ND
	Fall	4/13–4/30/97	-0.3 ± 1.2	7.19	-2.5 ± 8.9	ND	ND

[a]ND-not determined.

that the deficits measured at the end of the summer cruise would have nearly disappeared in the interval between the cruises, i.e. about three half-lives of ^{234}Th. In contrast, particulate export of ^{234}Th determined from the non-steady-state model is negligible at Orca during the spring and fall cruises. Stations Sei and Minke also show negligible fluxes during the fall, within the uncertainties. It is important to note that the errors on the values of P_{Th} calculated from Eq. (9) are significant. Greater measurement precision as well as increased depth resolution on the ^{234}Th profiles is needed to accurately resolve the steady-state and non-steady-state Th (as well as POC) fluxes.

4.2. Comparison of ^{234}Th-derived POC export fluxes with other estimates

An important parameter in oceanic carbon cycling is the ratio of export of POC on sinking particles to the primary production. This ratio, labeled the "*ThE*" ratio when determined by ^{234}Th (Buesseler, 1998), characterizes the POC flux to waters deeper than the euphotic zone and, depending on the extent of remineralization, to bottom sediments. During the spring cruise, primary production at station Orca was 33.9 ± 25.9 mmol C m^{-2} d^{-1} while Minke displayed 5.4 ± 2.3 mmol C m^{-2} d^{-1} (J. Marra, pers. comm., JGOFS Data Workshop, 1999). POC export based on ^{234}Th deficiencies is less than 10% of production at this time (Table 1). In contrast, during the summer cruise, primary production was 45.3 ± 1.2 at Orca, 88.5 ± 68.5 at Minke and 50 mmol C m^{-2} d^{-1} at Sei (J. Marra, pers. comm. JGOFS Data Workshop, 1999). Average steady-state POC fluxes derived from the summertime ^{234}Th profiles are ~ 44, 68 and 24% of these values at Orca, Minke and Sei, respectively. Primary production rates are low during the fall (mean ~ 3 mmol C m^{-2} d^{-1} at the three stations, J. Marra pers. comm., JGOFS Data Workshop, Keystone, CO, August 1999), and ^{234}Th-derived POC export declines to low values late in the fall.

Comparisons between ^{234}Th-derived POC export and productivity are compromised during a bloom by the fact that the maximum export flux frequently lags the maximum in production. This is well demonstrated in the Ross Sea. Primary production along the JGOFS AESOPS transect in the Ross Sea (Fig. 1) peaked in early December 1996, while POC inventories peaked about one month later (Smith et al., 2000, Gardner et al., 2000). The greatest rate of decline in POC inventories is over the course of the summer cruise. Smith et al. (2000) report POC inventories along the AESOPS transect over four weekly periods during the summer cruise. From an initial value of 4900 mmol C m^{-2} in the first week, the inventory decreases in the second week, increases in the third and then decreases to a low of 1940 mmol C m^{-2} by the fourth week (Smith et al., 2000). The net change over the cruise yields an average daily flux of ~ 150 mmol C m^{-2} d^{-1}. Further decreases in POC inventory occurred in the interval between the summer and fall cruises, and values are ~ 200 mmol C m^{-2} by the start of the fall cruise. POC is lost at an average rate of ~ 20 mmol C m^{-2} d^{-1} during this period.

Decreases in POC inventory correspond to both export and remineralization of organic matter. As indicated by the ^{234}Th-derived depth profiles of POC flux and the

floating sediment trap data of Asper and Smith (1999), remineralization of POC within the upper 100 m can result in about a factor of two attenuation of the flux. Indeed Asper and Smith (1999) estimated that about 50% of the total production was regenerated prior to export. The Th-derived estimates of POC flux during the summer cruise can be compared with the loss of POC documented by Smith et al. (2000) and Gardner et al. (2000). The latter was estimated along the AESOPS transect, and if we average our POC fluxes from Minke and Orca during the summer cruise, the export flux of POC is $\sim 40\,\mathrm{mmol\,C\,m^{-2}\,d^{-1}}$ (based on steady-state Th fluxes) or $\sim 70\,\mathrm{mmol\,C\,m^{-2}\,d^{-1}}$ (based on non-steady-state Th fluxes). This suggests that ~ 30–50% of the decline in POC standing crop is due to export while the remainder is likely remineralized. These values are consistent with the attenuation of the POC flux with depth, as determined in this study, and as seen in the sediment trap profiles of Asper and Smith (1999). Of the fraction of POC remineralized in the upper 100 m of the Ross Sea, Asper and Smith (1999) have suggested that bacterial activity is likely responsible. Dissolved organic matter shows the greatest increases during the summer, although the magnitude of DOC production is small compared with both production and changes in POC inventories (Carlson et al., 2000). Another potential pathway for diminishing phytoplankton biomass is through zooplankton grazing, although Caron et al. (2000) have demonstrated that microzooplankton grazing was quite low during the JGOFS cruises and could not have significantly affected phytoplankton standing stocks.

In contrast to the magnitude and timing of ^{234}Th-derived POC fluxes from the euphotic zone, POC fluxes measured in sediment trap moorings (200 and 500 m) at stations Orca and Minke show low values that attain maxima late during the time of the fall cruise, coincident with a large flux in pteropods to the traps (Collier et al., 2000). During late February 1997, POC fluxes recorded in the 200 m trap are $1.4\,\mathrm{mmol\,C\,m^{-2}\,d^{-1}}$ close to station Orca and $0.3\,\mathrm{mmol\,C\,m^{-2}\,d^{-1}}$ close to station Sei (Collier et al., 2000). Higher POC fluxes (6–12 $\mathrm{mmol\,C\,m^{-2}\,d^{-1}}$) in the southern Ross Sea were reported for late February 1990 by Dunbar et al., (1998). In addition to interannual variations in productivity, differences between sediment trap deployments in different years may be explained by the nature of the settling material: diatom frustules and associated organic matter may be transferred more efficiently to depth than *Phaeocystis* colonies, which may disaggregate during sinking.

Taken together, the JGOFS results from the summer cruise indicate that ~ 30–50% of the change in POC inventory in the upper 100 m is exported below this depth, but $< 4\%$ of that fraction is collected in traps at 200 m. A similar view of organic carbon cycling in the Ross Sea was presented by Nelson et al. (1996). Their budget, based on measurements of production, water column fluxes and benthic regeneration and accumulation, suggests that $\sim 40\%$ of the production is exported from the euphotic zone, 3% survives to 250 m and only 0.2% is accumulated in bottom sediments. Similar large offsets in POC flux have been observed in other high latitude ecosystems such as the Northeast Water Polynya off Greenland (Cochran et al., 1997) and suggest that efficient recycling of organic material may be common in such systems.

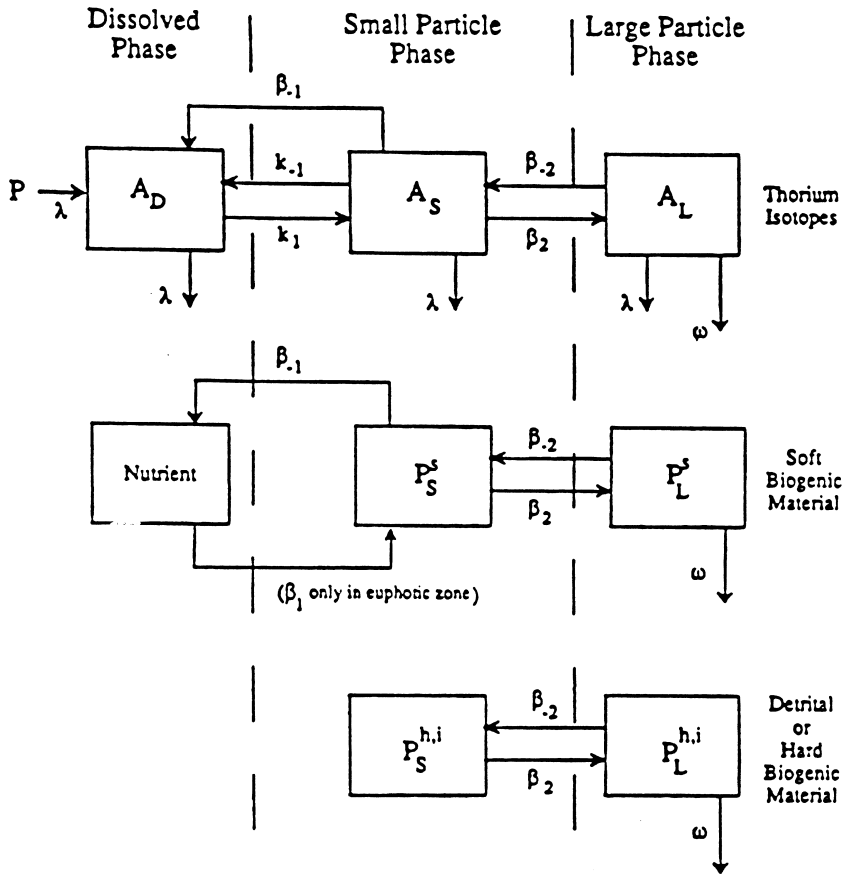

Fig. 11. Box model of particle and thorium cycling in the ocean. β_2, β_{-2}, β_{-1}, β_1, k_1 and k_{-1} are first-order rate constants pertaining to particle aggregation, particle disaggregation, remineralization, biogenic particle formation, thorium adsorption and desorption respectively; A_D, A_s, and A_L are thorium activities (dpm l^{-1}) in solution, small (1–70 μm) and large (> 70 μm) particles, respectively; P is thorium production from dissolved U or Ra; P_s and P_L are small and large particle concentrations (g l^{-1}). (Superscripts s, h and I denote soft biogenic material, tests or shells and detrital particles, respectively). ω is the sinking velocity of large particles. Adapted from Cochran et al. (1993).

4.3. Particle aggregation and disaggregation rates

Thorium isotopes offer the opportunity to characterize aggregation and disaggregation rates of particles in marine systems. Both ^{234}Th and ^{228}Th are short-lived and respond to temporal changes in scavenging, albeit somewhat differently because of the difference in their half-lives and rates of production. One approach for characterizing particle dynamics from these tracers is that described by Cochran et al. (1993) and

Murnane et al., (1996) and is illustrated in the simplified scavenging model shown in Fig. 11. The large and small particle reservoirs are assumed to exchange thorium and mass via aggregation and disaggregation. These processes are taken as first-order, characterized by rate constants β_2 and β_{-2}, respectively. The equation describing the large particle pool (Fig. 11) is

$$\partial A_L/\partial t = A_s\beta_2 - A_L(\beta_{-2} + \lambda) - \omega(\partial A_L/\partial z) + V, \tag{10}$$

where A_L and A_s are Th activities on large and small particles, respectively, β_2 and β_{-2} are the aggregation and disaggregation rate constants, λ is the Th decay constant, ω is the particle sinking velocity, and V corresponds to advective and diffusive transport. Eq. (10) may be solved for β_2 as

$$\beta_2 = m\beta_{-_2} + b, \tag{11}$$

where m is A_L/A_s and b is $[\partial A_L/\partial t + A_L\lambda - \omega(\partial A_L/\partial z) + V]/A_s$. As described above, we lack sufficient spatial resolution in Th profiles to evaluate V. However, prior application of Eq. (10) under bloom conditions (Buesseler et al., 1992a; Cochran et al., 1993), as well as the analysis by Jaeger et al., (1996) of lateral particle transport in the southern Ross Sea, suggests that the local vertical flux gradient term is dominant and we neglect V in the calculations that follow.

We apply Eq. (10) to the ^{234}Th and ^{228}Th data from station Orca by dividing the water column into depth intervals based on the sampling depths and calculate values corresponding to m and b for each isotope. A sinking velocity of large particles must be chosen and we set it at 150 m d^{-1} for comparison with previous studies (Cochran et al., 1993; Murnane et al., 1996). However, this value is consistent with experimentally measured settling velocities of trapped material near station Orca ($\sim$ 60–190 m d^{-1}, Jaeger et al., 1996). Values of β_2 and β_{-2} vary directly with sinking velocity, and thus trends with depth or time will be qualitatively similar regardless of the value of ω used.

The flux gradient term in b is generally much larger than either the decay term or the temporal term. For example, considering the depth interval comprising the upper 30 m at station Orca, the flux gradient of ^{234}Th on large sinking particles ($\omega\partial A_L/\partial z$) varies from -25.2×10^{-3} to 1.32×10^{-3} dpm l^{-1} d^{-1} between the spring and summer cruises. Over the same interval, the decay term ($A_L\lambda$) varies from 9×10^{-5} to 1.1×10^{-4} dpm l^{-1} d^{-1} and the temporal term ($\partial A_L/\partial t$) is 1.1×10^{-5} dpm l^{-1} d^{-1}. A similar situation obtains for ^{228}Th; the flux gradient ranges from -1.2×10^{-3} to -1.1×10^{-3} dpm l^{-1} d^{-1}, the decay term ranges from 1.0×10^{-4} to 1.7×10^{-4} dpm l^{-1} d^{-1} and the temporal term is 1.0×10^{-6} dpm l^{-1} d^{-1}. Accordingly, we neglect the temporal term in using (9) to evaluate b.

The approach for calculating β's involves simultaneous solution of two forms of Eq. (10), one for ^{228}Th and one for ^{234}Th. Solution for β_2 and β_{-2} is possible once a value of particle sinking velocity is set. The slopes of the relationships are the ratio of large particle to small particle thorium activity. These values tend to be <0.3 for ^{234}Th and >0.3 for ^{228}Th. We apply Eq. (10) in a pair-wise fashion to adjacent depths in the profiles of particulate ^{234}Th and ^{228}Th. The results are sensitive to

Table 3
Particle aggregation (β_2) and disaggregation (β_{-2}) rate constants and POC aggregation and disaggregation rates calculated from ^{234}Th and ^{228}Th at station Orca

Cruise	Depth interval (m)	Aggregation (β_2) (d^{-1})	Disaggregation (β_{-2}) (d^{-1})	POC (> 70 μm) ($\mu mol\ l^{-1}$)	POC (1–70 μm) ($\mu mol\ l^{-1}$)	POC aggregation ($\mu mol\ l^{-1}\ d^{-1}$)	POC disaggregation ($\mu mol\ l^{-1}\ d^{-1}$)
Spring	ORCA-2 (11/2/96[a])						
	10–30	0.48 ± 16	13.8 ± 13.6	0.080	0.389	0.19	1.1
	80–105	0.64 ± 7.4	11.2 ± 9.8	0.124	0.358	0.14	1.4
	205–305	0.12 ± 0.17	2.6 ± 1.1	0.019	0.080	0.01	0.05
Summer	ORCA-1 (1/19/97[a])						
	5–30	0.20 ± 1.2	7.2 ± 6.3	0.016	0.871	0.17	1.1
	ORCA-2 (2/1/97[a])						
	30–55	0.97 ± 0.04	0.39 ± 0.31	1.63	0.585	0.57	0.63
	55–205	0.29 ± 0.37	1.2 ± 1.1	1.18	0.442	0.13	1.4
Fall	ORCA-1 (4/14/97[a])						
	65–82.5	0.78 ± 0.53	7.7 ± 2.0	0.011	0.073	0.06	0.09
	ORCA-2 (4/23/97[a])						
	5–15	0.04 ± 0.30	6.5 ± 4.5	0.038	0.085	0.003	0.24
	50–75	0.14 ± 0.15	2.8 ± 1.9	0.014	0.104	0.002	0.04

[a]mm/dd/yy.

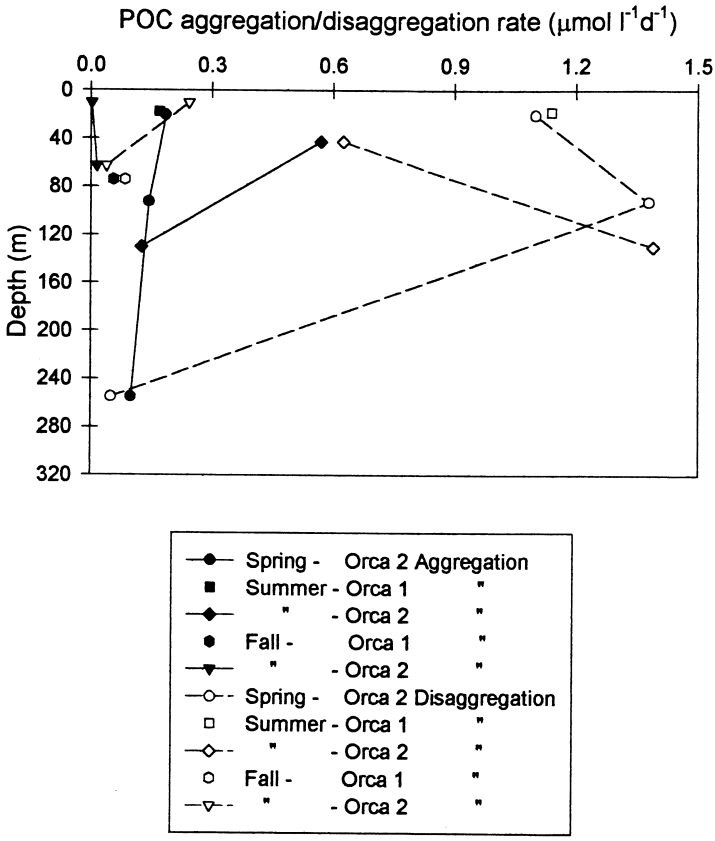

Fig. 12. POC aggregation (closed symbols) and disaggregation rates (open symbols) vs. depth in the water column at Station Orca.

errors in both the ^{234}Th and ^{228}Th activities on small and large particles at the two depths. As a consequence, the uncertainties in the slopes as well as in the flux gradients can be significant and can cause the calculated values of β_2 and β_{-2} to be negative. This is a physical impossibility and, as pointed out by Murnane et al. (1996), can arise by combining a large uncertainty with the assumption that the rate constants have normal probability distributions. Use of a lognormal probability distribution precludes negative values and is a better approximation of the actual probability distribution of these parameters. For an initial look at the possible trends in aggregation and disaggregation at station Orca, we focus on instances in which both β_2 and β_{-2} are positive. Values of β_2 range from 0.04 to 0.20 d^{-1} and β_{-2} ranges from 2.4 to 13.8 d^{-1}. These values are greater than those determined by Cochran et al. (1993) and Murnane et al. (1996) for the North Atlantic Bloom Experiment (0.003–0.09 d^{-1} for

β_2 and 0.34–1.1 d^{-1} for β_{-2}, over the course of the spring bloom), but less than those estimated by Dunne et al. (1997) in 0–100 m of the equatorial Pacific ($\sim$ 0.9–3.5 d^{-1} for β_2). The difference may reflect differences in the processes that contribute to aggregation and disaggregation of particles during blooms at the different sites, differences in settling velocity as well as differences in the energy of shelf vs. open ocean environments. However, an additional factor is that the North Atlantic results correspond to depths of 150–300 m while the Ross Sea results generally focus on the upper 100 m of the water column. Indeed, values of 0.12 d^{-1} for β_2 and 2.6 d^{-1} β_{-2} are calculated for station Orca between 205 and 305 m (Table 3), values that are more comparable to the North Atlantic results.

Fluxes of aggregation and disaggregation may be calculated by multiplying the appropriate rate constant by the concentrations of small or large particles. We use the POC concentrations determined from the in situ pump filters for this purpose (Table 3). The results show that aggregation of POC is greatest in the upper 50 m and decreases with depth (Fig. 12). POC aggregation rates in the upper 100 m increase from spring to summer and reach maximum values late in the summer cruise. Disaggregation rates of POC show an inverse pattern, decreasing with time. During the spring and summer cruises, POC disaggregation rates increase to a maximum at $\sim$ 150 m and decrease to low values at deeper depths.

These trends are most pronounced during the time interval represented by austral spring – summer (Fig. 12). The increase in the aggregation rate of POC is accompanied by a decrease in disaggregation rate during the second occupation of Orca during the summer cruise, and is consistent with the elevated POC in the large particle fraction at that time (Fig. 6a). At all other times, disaggregation dominates aggregation, although the absolute rates decrease as the bloom subsides.

The changes in the rates of POC aggregation and disaggregation can be considered in the context of the phytoplankton assemblage at station Orca and zooplankton grazing effects. The latter could cause aggregation of particles through fecal pellet formation, but Caron et al. (2000) documentes that rates of grazing by the microzooplankton were low and insufficient to affect phytoplankton standing stocks during the JGOFS cruises. In the south-central Ross Sea, blooms of the nonsiliceous colonial haptophyte *Phaeocystis* are common (Leventer and Dunbar, 1996). This species occurs initially as small motile cells that aggregate into large, rapidly sinking colonies. Late in *Phaeocystis* blooms, the colonies can sink and disaggregate (Wassmann, 1994). Mathot et al. (1999) found that *Phaeocystis* cells were abundant within the nanoplankton in the southern Ross Sea in during the spring (October) and that the colonial stage was common in the microplankton during the summer. This pattern is consistent with the trend in aggregation and disaggregation of POC at station Orca: increases in aggregation of POC in the euphotic zone during the summer cruise, coupled with decreases in disaggregation. Enhanced disaggregation at $\sim$ 100–150 m may result from breakup of sinking colonies of *Phaeocystis*. The individual *Phaeocystis* cells will likely settle more slowly, and this phenomenon may help explain the low POC fluxes measured in sediment traps at 200 m. Moreover, the disaggregated *Phaeocystis* cells are subject to grazing, decomposition or advective transport out of the area.

5. Summary

Depth profiles of ^{234}Th from stations Minke, Orca and Sei show a pattern typical of the development and progression of a phytoplankton bloom. Little scavenging was evident in the upper 100 m of the water column in the early spring. Removal increased through the austral summer and decreased into the fall. Application of a non-steady-state model to the Th profiles suggests that Th scavenging is significant during the summer cruise and in the interval between the summer and fall cruises (early February to mid-April). Average POC fluxes through 100 m during the summer cruise (estimated from a steady state Th model) are ~ 60 mmol m^{-2} d^{-1} at station Minke (1/13–2/8/97), ~ 20 mmol m^{-2} d^{-1} at Orca (1/19–2/1/97) and ~ 12 mmol m^{-2} d^{-1} at Sei (1/24/97). POC fluxes calculated using a non-steady state model applied to the summer ^{234}Th data are 85 mmol C m^{-2} d^{-1} at Minke (1/13–2/8/97) and 50 mmol C m^{-2} d^{-1} at Orca (1/19–2/1/97). The decrease in POC inventories along the AESOPS transect in the southern Ross Sea is ~ 150 mmol C m^{-2} d^{-1} during the summer cruise (Gardner et al., 2000), and the Th-derived POC export fluxes at stations Orca and Minke average about 30–50% of this value. The remainder of the decline in POC inventory is likely due to remineralization. This result is consistent with depth profiles of POC flux estimated from ^{234}Th profiles suggesting that POC flux decreases by 50–80% from maximum values in the upper 100 m. Less than 4% of the POC export fluxes estimated from ^{234}Th are recorded in Ross Sea sediment traps at 200 m (Collier et al., 2000).

Coupling ^{234}Th and ^{228}Th data on small (1–70 μm) and large ($>$ 70-μm) particles permits estimation of the rates of POC aggregation and disaggregation. POC aggregation rates decrease with depth while disaggregation rates increase. Rates of both processes are low below 200 m. Subsurface aggregation rates are at a maximum late in the summer while disaggregation rates are low at this time. The production of large sinking aggregates during the summer cruise is consistent with the maximum fluxes of POC and ^{234}Th from the upper 100 m observed at that time. Moreover, increases in POC disaggregation rate with depth may help explain the low POC fluxes recorded in sediment traps compared with export from the upper 100 m as sinking particles disaggregate before they reach the trap depth.

Acknowledgements

We thank the officers and crew of the R/V *Nathaniel B. Palmer* and support personnel from Antarctic Support Associates for their assistance. Without their help, this study would not have been possible. We are grateful to Ellen Roos and Eileen Goldsmith for their assistance with the field work and logistics. This research has benefited from numerous discussions with our colleagues, including J. Dymond, W. Gardner, W. Smith and I. Walsh. Reviews by R. Anderson, D. DeMaster, J. Dunne and M. Rutgers van der Loeff improved the manuscript. Portions of this work constitute the MS thesis of Hong-Wei Wang, SUNY-Stony Brook. This research was supported by the National Science Foundation as part of the Joint Global Ocean

Flux Study (grants OPP-9530861 to KOB and MPB and OPP-9612761 to JKC); we gratefully acknowledge this support. This is Contribution Number 1200 from the Marine Sciences Research Center, 10252 from the Woods Hole Oceanographic Institution and JGOFS Number 564.

References

Altabet, M.A., Bishop, J.K.B., McCarthy, J.J., 1992. Differences in particulate nitrogen concentration and isotopic composition for samples collected by bottles and large-volume pumps in Gulf Stream warm-core rings in the Sargasso Sea. Deep-Sea Research I 39, S405–S417.

Asper, V.L., Smith Jr., W.O., 1999. Particle fluxes during austral spring and summer in the southern Ross Sea, Antarctica. Journal of Geophysical Research 104, 5345–5359.

Bacon, M.P., Cochran, J.K., Hirschberg, D., Hammar, T.R., Fleer, A.P., 1996. Export flux of carbon at the equator during the EqPac time-series cruises estimated from ^{234}Th measurements. Deep-Sea Research II 43, 1133–1153.

Bishop, J.K.B., Schpack, D., Sherrel, R.M., Conte, M., 1985. A multiple-unit large-volume filtration system for sampling oceanic particulate matter in mesoscale environments. In: Zirino, A. (Ed.), Mapping Strategies in Chemical Oceanography, Advances in Chemistry Series No. 209. American Chemical Society, Washington, DC, pp. 155–175.

Buesseler, K.O., 1998. The decoupling of production and particulate export in the surface ocean. Global Biogeochemical Cycles 12, 297–310.

Buesseler, K.O., Andrews, J.A., Hartman, M.C., Belastock, R., Chai, F., 1995. Regional estimates of the export flux of particulate organic carbon derived from ^{234}Th during the JGOFS EqPac program. Deep-Sea Research II 42, 777–804.

Buesseler, K.O., Bacon, M.P., Cochran, J.K., Livingston, H.D., 1992a. Carbon and nitrogen export during the JGOFS North Atlantic Bloom Experiment estimated from ^{234}Th : ^{238}U disequilibrium. Deep-Sea Research I 39, 1115–1137.

Buesseler, K., Ball, L., Andrews, J., Benitez-Nelson, C., Belastock, R., Chai, F., Chao, Y., 1998. Upper ocean export of particulate organic carbon in the Arabian Sea derived from thorium-234. Deep-Sea Research II 45, 2461–2487.

Buesseler, K.O., Cochran, J.K., Bacon, M.P., Livingston, H.D., Casso, S.A., Hirschberg, D., Hartman, M.C., Fleer, A.P., 1992b. Determination of thorium isotopes in seawater by non-destructive and radiochemical procedures. Deep-Sea Research I 39, 1103–1114.

Carlson, C.A., Hansell, D.A., Peltzer, E.T., Smith, Jr., W.O., 2000. Stocks and dynamics of dissolved and particulate organic matter in the southern Ross Sea, Antarctica. Deep-Sea Research II 47, 3201–3225.

Caron, D.A., Dennett, M.R., Lonsdale, D.J., Moran, D.M., Shalapyonok, L. 2000. Microzooplankton herbivory in the Ross Sea, Antarctica. Deep-Sea Research II 47, 3249–3272.

Charette, M.A., Moran, S.B., 1999. Rates of particle scavenging and particulate organic carbon export estimated using ^{234}Th as a tracer in the subtropical and equatorial Atlantic Ocean. Deep-Sea Research II 46, 885–906.

Chen, J.H., Edwards, R.L., Wasserburg, G.J., 1986. ^{238}U, ^{234}U and ^{232}Th in seawater. Earth Planetary Science Letters 80, 241–251.

Clegg, S.L., Bacon, M.P., Whitfield, M., 1991. Application of a generalized scavenging model to thorium isotope and particle data at equatorial and high-latitude sites in the Pacific Ocean. Journal of Geophysical Research 96, 20655–20670.

Clegg, S.L., Whitfield, M., 1991. A generalized model for the scavenging of trace metals in the open ocean II, Thorium Scavenging. Deep-Sea Research I 38, 91–120.

Coale, K.H., Bruland, K.W., 1987. Oceanic stratified euphotic zone as elucidated by ^{234}Th : ^{238}U disequilibria. Limnology and Oceanography 32, 189–200.

Cochran, J.K., Barnes, C., Achman, D., Hirschberg, D.J., 1995. Thorium-234/Uranium-238 disequilibrium as an indicator of scavenging rates and particulate organic carbon fluxes in the Northeast Water Polynya, Greenland. Journal of Geophysical Research 100, 4399–4410.

Cochran, J.K., Buesseler, K.O., Bacon, M.P., Livingston, H., 1993. Thorium isotopes as indicators of particle dynamics in the upper ocean: results from the JGOFS North Atlantic Bloom Experiment. Deep-Sea Research I 40, 1569–1595.

Cochran, J.K., Roberts, K.A., Barnes, C., Achman, D., 1997. Radionuclides as indicators of particle and carbon dynamics on the East Greenland Shelf. Radioprotection – Colloques 32 (c2), 129–136.

Collier, R., Dymond, J., Honjo, S., Manganini, S., Francois, R., Dunbar, R., 2000. The vertical flux of biogenic and lithogenic material in the Ross Sea: moored sediment trap observations 1996–1998. Deep-Sea Research II 47, 3491–3520.

DeMaster, D.J., Dunbar, R.B., Gordon, L.I., Leventer, A.R., Morrison, J.M., Nelson, D.M., Nittrouer, C.A., Smith Jr., W.O., 1992. Cycling and accumulation of biogenic silica and organic matter in the high-latitude environments: the Ross Sea. Oceanography 5, 146–153.

DeMaster, D.J., Ragueneau, O., Nittrouer, C.A., 1996. Preservation efficiencies and accumulation rates for biogenic silica and organic C, N, and P in high latitude sediments: the Ross Sea. Journal of Geophysical Research 101, 18501–18518.

Dunbar, R.B., Leventer, A.R., Mucciarone, D.A., 1998. Water column sediment fluxes in the Ross Sea, Antarctica: atmospheric and sea ice forcing. Journal of Geophysical Research 103, 30741–30759.

Dunne, J.P., Murray, J.W., Young, J., Balistrieri, L.S., Bishop, J., 1997. ^{234}Th and particle cycling in the central equatorial Pacific. Deep-Sea Research II 44, 2049–2083.

El-Sayed, S.Z., Biggs, D.C., Holm-Hansen, O., 1983. Phytoplankton standing crop, primary productivity, and near-surface nitrogenous nutrient fields in the Ross Sea Antarctica. Deep-Sea Research I 30, 871–886.

Gardner, W.D., Richardson, M.J., Smith, W.O. Jr. 2000. Seasonal patterns of water column particulate organic carbon and fluxes in the Ross Sea, Antarctica, Deep-Sea Research II 47, 3423–3449.

Gustafsson, O., Buesseler, K.O., Geyer, W.R., Moran, S.B., Gschwend, P.M., 1998. An assessment of the relative importance of horizontal and vertical transport of particle-reactive chemicals in the coastal ocean. Continental Shelf Research 18, 805–829.

Jacobs, S.S., Amos, A.F., Bruchhausen, P.M., 1970. Ross Sea oceanography and Antarctic Bottom Water formation. Deep-Sea Research I 17, 935–962.

Jaeger, J.M., Nittrouer, C.A., DeMaster, D.J., Kelchner, C., Dunbar, R.B., 1996. Lateral transport of settling particles in the Ross Sea and implications for the fate of biogenic material. Journal of Geophysical Research 101, 18749–18788.

Langone, L., Frignani, M., Cochran, J.K., Ravaioli, M., 1997. Scavenging processes and export fluxes close to a retreating seasonal ice margin (Ross Sea Antarctica). Water Air and Soil Pollution 99, 705–715.

Ledford-Hoffman, P.A., DeMaster, D.J., Nittrouer, C.A., 1986. Biogenic silica accumulation in the Ross Sea and the importance of Antarctic Continental-shelf deposits in the marine silica budget. Geochimica Cosmochimica Acta 50, 2099–2110.

Leventer, A., Dunbar, R.B., 1996. Factors influencing the distribution of diatoms and other algae in the Ross Sea. Journal of Geophysical Research 101, 18489–18500.

Livingston, H.D., Cochran, J.K., 1987. Determination of transuranic and thorium isotopes in ocean water: in solution and filterable particles. Journal of Radioanalytical and Nuclear Chemistry 115, 299–308.

Mathot, S., Dennett, M.R., Smith Jr., W.O., Caron, D.A., Brown, K.J., Moran, D.M., Pardini, A., Shalapyonok, L., 1999. Nano- and micro-phytoplankton abundance and biomass in the Ross Sea, Antarctica: an AESOPS study EOS, Transactions. American Geophysical Union 80, 266.

Moran, S.B., Charette, M.A., Pike, S.M., Wicklund, C.A., 1999. Difference in seawater particulate organic carbon concentration in samples collected using small-volume and large-volume methods: the importance of DOC adsorption to the filter blank. Marine Chemistry 67, 33–42.

Murnane, R.J., Cochran, J.K., Sarmiento, J.L., 1994. Estimates of particle- and thorium-cycling rates in the northwest Atlantic Ocean. Journal of Geophysical Research 99, 3373–3392.

Murnane, R.J., Cochran, J.K., Buesseler, K.O., Bacon, M.P., 1996. Least squares estimates of thorium, particle, and nutrient cycling rate constants from the JGOFS North Atlantic Bloom Experiment. Deep-Sea Research I 43, 239–259.

Murray, J.W., Downs, J.N., Strom, S., Wei, C.-L., Jannasch, H.W., 1989. Nutrient assimilation, export production and ^{234}Th scavenging in the eastern equatorial Pacific. Deep-Sea Research I 36, 1471–1489.

Murray, J.W., Young, J., Newton, J., Dunne, J., Chapin, T., Paul, B., 1996. Export flux of particulate organic carbon from the central equatorial pacific determined using a combined drifting trap-^{234}Th approach. Deep-Sea Research II 43, 1095–1132.

Nelson, D.M., DeMaster, D.J., Dunbar, R.B., Smith Jr., W.O., 1996. Cycling of organic carbon and biogenic ilica in the Southern Ocean: Estimates of water-column and sedimentary fluxes on the Ross Sea continental shelf. Journal of Geophysical Research 101, 18519–18532.

Rutgers van der Loeff, M.M., 1994. ^{228}Ra and ^{228}Th in the Weddell Sea. In: The Polar Oceans and Their Role in Shaping the Global Environment, Geophysical Monograph 85. American Geophysical Union, Washington, DC, pp. 177–186.

Smith Jr., W.O., Nelson, D.M., DiTullio, G.R., Leventer, A.R., 1996. Temporal and spatial patterns in the Ross Sea : Phytoplankton biomass, elemental composition, productivity and growth rates. Journal of Geophysical Research 101, 18455–18465.

Smith Jr., W.O., Marra, J., Hiscock, M., Barber, R.T. 2000. The seasonal cycle of phytoplankton biomass and primary productivity in the Ross Sea, Antarctica. Deep-Sea Research II 47, 3119–3140.

Wassmann, P., 1994. Significance of sedimentation for the termination of Phaeocystis blooms. Journal of Marine Systems 5, 81–100.

Yager, P.L., Wallace, D.W.R., Johnson, K.M., Smith Jr., W.O., Minnett, P.J., Deming, J.W., 1995. The Northeast Water Polynya as an atmospheric CO_2 sink: a seasonal rectification hypothesis. Journal of Geophysical Research 100 (C3), 4389–4398.